Changes in Streamflow Statistical Structure across the United States due to Recent Climate Change

Abhinav Gupta[*1], Rosemary W. H. Carroll[2], Sean A. McKenna[2]

[1]Division of Hydrologic Sciences, Desert Research Institute, 755 E. Flamingo Rd., Las Vegas, NV, 89119, United States of America
[2]Division of Hydrologic Sciences, Desert Research Institute, 2215 Raggio Pkwy, Reno, NV 89512, United States of America

[*]Corresponding Author: Abhinav Gupta (abhinav.gupta@dri.edu)
Rosemary W. H. Carroll: rosemary.carroll@dri.edu
Sean A. McKenna: sean.mckenna@dri.edu

****This is a non-peer reviewed preprint submitted to EarthArXiv. This paper has been submitted to the *Journal of Hydrology* for peer-review.**

Highlights

(1) Changes in streamflow statistical structure (SSS) occurred in the watersheds across the USA
(2) Change in climatic statistics appears to be one of the causes of the changes in the SSS
(3) Landscape characteristics play an important but secondary role in changing SSS
(4) Increase in winter temperature increases (decreases) the high-frequency component of streamflow in arid (humid) regions

Abstract:

A variety of watershed responses to climate change are expected due to non-linear interactions between various hydrologic processes acting at different timescales that are modulated by watershed properties. Changes in statistical structure (spectral properties) of streamflow in the USA due to climate change were studied for water years 1980-2013. The Fractionally differenced Autoregressive Integrated Moving Average (FARIMA) model was fit to the deseasonalized streamflow time series to model its statistical structure. FARIMA allows the separation of streamflow into low- (slowly varying) and high-frequency (fast varying) components. Results show that in the snow-dominated watersheds, the contribution of low-frequency components to total streamflow variance decreased over the study period, and the contribution of high-frequency components increased. The change in the snow-dominated watersheds was primarily driven by changes in rainfall statistics and changes in snow water equivalent but also by changes in seasonal temperature statistics. Among the rain-driven watersheds, the contribution of high-frequency components generally increased in arid regions but decreased in humid regions. In both humid and arid rain-driven watersheds, increasing winter temperature appears to be responsible for the change in streamflow statistical structure. These results have consequences for predictability of streamflow in the presence of climate change. We expect that changes in the high-frequency component will result in decreased predictability of streamflow. Further, the analysis carried out in this study allows to understand the plausible changes in watershed hydrologic processes that affect streamflow without using process-based or conceptual models.

Keywords: Streamflow, Climate change, FARIMA, Spectral analysis, snow-dominated watersheds, Rain-driven watersheds

1. Introduction

1.1 Background

The global hydrologic water balance will be impacted directly by climate change (Milly et al., 2005; Milly & Dunne, 2016; Mote et al., 2018; Manabe & Broccoli, 2020) which will alter streamflows. The extent and nature of hydrologic change depends upon several factors including watershed geomorphological characteristics (Lee & Delleur, 1972; Rodriguez-Iturbe & Rinaldo, 1997, Chap. 7), vegetation characteristics and soil properties (Eagleson, 1978), the dominant mode of streamflow production (snowmelt or rain, quick flow, baseflow etc.), changes in vegetation characteristics (e.g., Milly, 1997), and the pre-existing climate against which changes occur. Thus, a rich variety of watershed responses can be expected due to the change in climate as summarized through climate statistics (Gordon et al., 2022). The hydrologic responses of watersheds to climate change need to be understood to devise an effective adaption strategy.

Because of strong feedbacks between various components of a hydrologic systems, climate change can potentially lead to profound changes in watershed hydrologic regime. Hydrologic regime here refers to the interaction between different components of hydrologic process which produce hydrologic fluxes such as streamflow and evapotranspiration (ET). An example is the feedback between climate, soil, and vegetation properties (Rodriguez-Iturbe et al., 1999, 2001). Soil stores some of the precipitation as soil moisture which is taken up by the vegetation (Porporato et al., 2001). Climate has a strong control over soil moisture dynamics via precipitation frequency and depth (Laio et al., 2001). Also, the intensity of the climatic control on soil moisture dynamics is directly affected by soil properties such as soil texture, soil depth, and water holding capacity. Vegetation provides feedback to the atmospheric properties via transpiration and, at long timescales, soil properties via plant residue decomposition in soils (Eagleson, 1982). Thus, vegetation properties influence climate through the soil zone. These feedbacks operate at different timescales. The feedback between climate and soil moisture dynamics is fastest, followed by the feedback between climate and vegetation (via soil moisture dynamics). The feedback between vegetation and soil properties is slowest. Therefore, effects of climate change are expected to be observable at different timescales.

Streamflow is the integrated response of a watershed's hydrology, which is affected by inherent properties such as soil depth and texture, bedrock permeability, and topography that influence hydrology. Thus, studying changes in streamflow characteristics provides the clues to understanding the changes in watershed hydrologic regime. Hydrologists have employed various mathematical models (simulation approaches) to understand the streamflow response of a watershed at different timescales. These models can be broadly classified as deterministic models (Beven, 2011), stochastic models (Klemeš, 1978), and statistical models (Montanari et al., 1997). The model that is used depends upon the spatial scale (watershed scale, regional scale, global scale, etc.) and timescale (daily, monthly, yearly, etc.) at which simulations/predictions are required along with the purpose of simulations/predictions (policy making, scientific hypothesis testing).

For most of the models used, some parameters of the model need to be calibrated against observations. The values that these parameters take depends upon climate statistics (mean annual precipitation depth, precipitation frequency, seasonal mean temperatures etc.) and watershed properties. Temporal non-stationarity introduced by climate change (Milly et al., 2008) makes the calibrated parameters dependent upon observation time-period. In fact, climate change may directly affect the physical characteristics of a watershed via change in vegetation characteristics (Milly, 1997). This introduces additional uncertainty in model projections/predictions in the presence of climate change. For example, Stephens et al. (2020) showed that changes in rainfall statistics along with changes in atmospheric CO_2 can change the soil moisture statistics. It may take a few years for a calibrated hydrologic model to adjust to the new equilibrium conditions. Other examples of climate change impacting watershed hydrologic characteristics include changes in snowpack in the western USA (e.g., Knowles et al., 2006; Mote et al., 2005; Mote, 2006; Belmecheri et al., 2016; Berg & Hall, 2017), and change in baseflow and stormflow (e.g., Ficklin et al., 2016). In summary, the problem is that climate non-stationarities may make a hydrologic model calibrated and validated against historical observations unreliable for prediction/simulation in changed conditions.

Some strategies have been proposed to address this problem. Klemeš (1986) proposed differential split-sample testing to test the robustness of a model under change, but such strategies may not be useful in case of large changes, especially if the change in a watershed is toward a drier hydrologic regime (Stephens et al., 2020). Singh et al. (2011) proposed a space-time symmetry approach under an uncertainty framework to estimate streamflows in a watershed in the presence of regime change. The idea behind space-time symmetry is to use available hydrologic information across different watersheds to predict future streamflow in another watershed. The assumption is that the spatial variability in hydro-climatological characteristics across watersheds is a good representation of the temporal variability that can be expected due to climate change. The idea of space-time symmetry has been demonstrated to be useful at yearly timescale using the Budyko framework (e.g., Sivapalan et al., 2011). Success of machine learning (ML) methods in estimating streamflows at gauged and ungauged locations at a daily timescale (Kratzert et al., 2018) suggests that there is a considerable amount of hydrologic information shared between different watersheds. However, there is limited evidence of successful application of space-time symmetry at a daily timescale (see, Singh et al., 2011), especially under a changing climate. Therefore, there is a need to further test this idea at daily timescale. Such a testing procedure would require identifying watersheds that have undergone hydrologic regime change. This is the main motivation for this work.

1.2 Streamflow Statistical Structure and objectives of the study

In this study, change in the streamflow statistical structure (SSS) was studied. We assume that a significant change in a watershed's hydrologic regime will result in a significant change in the SSS. Recently, it has been shown that SSS is also indicative of streamflow dynamics to some extent (Betterle et al., 2019) which further justifies studying the changes in SSS to understand the effect of climate change on hydrologic regime. Further, studying the changes in SSS can help identify the changes in flow paths and strengthening/weakening of different flow paths in a watershed using just available streamflow data. This is another motivation for this work.

Streamflow time series typically exhibit long-term persistence (Hurst, 1951) meaning that autocorrelations in streamflow decrease very slowly with time-lag. Studying the statistical structure of a stationary time series is equivalent to studying its spectral properties. Previous work has shown that the power spectral density (PSD) of streamflow scales linearly on log-log graph (Tessier et al., 1996), that is, $h(\omega) \propto \omega^{-\alpha_{\mathrm{h}}}$, where $h(\omega)$ denotes PSD at angular frequency $\omega[T^{-1}]$ and α_{h} denotes the slope of the scaling relationship. Also, a typical streamflow time series exhibits two scaling regimes (two different values of α_{h}) with scale break occurring between 1-20 days (Hirpa et al., 2010). Kim et al., (2016) and Yang & Bowling (2014) analyzed the changes in streamflow PSD to study the effects of urbanization on hydrologic regime in the South Korean watersheds and the Great Lakes region, respectively. Specifically, Kim et al. (2016) studied the changes in the slopes of two scaling regimes and the change in scale break point. Bras & Rodriguez-Iturbe (1993) and Chow et al. (1978) also illustrated the usefulness of spectral analysis in streamflow time series analysis. Gudmundsson et al. (2011) studied the contribution of low-frequency component (greater than 1-year timescale) to total streamflow variance in several

European watersheds but did not examine the change in the high-frequency component over time. Similarly, Zaerpour et al. (2021) defined streamflow regime based annual flow characteristics and high-frequency fluctuations were neglected. A systematic analysis of the changes in SSS over time across the contiguous USA has not been reported, to the best of authors' knowledge.

The objectives of this study are as follows:

(1) To conduct a spectral analysis of streamflow time series in watersheds across USA,
(2) To identify temporal changes in those spectral signatures
(3) To identify the spatial patterns of changes in SSS, and
(4) To investigate the relationship between SSS change, climatic statistics (such as annual mean temperature and rainfall), and watershed attributes.

Other researchers have studied the changes in hydrologic regime due to climate change, but their focus has been toward a few of the hydrologic processes or fluxes such as baseflow, soil moisture, annual streamflow etc. (e.g., Ficklin et al., 2016). Studying the change in spectral properties of streamflow time series can provide holistic insight into changes in hydrologic regime because:

(1) streamflow is an integrated response of the several hydrologic processes.
(2) To some extent, studying the changes in spectral properties allow us to understand the changes in various hydrologic flow paths. For example, changes in the low-frequency components of a streamflow time series can inform us about the changes in baseflow and snowmelt processes. Changes in the high-frequency components can inform us about the changes in soil moisture, surface flow, and interflow processes.

The changes in SSS can occur due to changes in climatic statistics and/or changes in watershed characteristics (such as changes in vegetation characteristics due to fire or forest die-offs by bark beetle). These factors interact with each other non-linearly and may even cancel each-other's effect (Boisrame et al., 2017). Therefore, it is likely that watershed that are close to each other in space, may exhibit different changes in SSS even though the effect of climate on the watersheds is similar. In this scenario, analysis across large number of watersheds provides a more realistic and holistic understanding.

Thus, this work aims to contribute to our understanding of the impact of climate change on hydrologic regime and hydrologic flow paths.

Another feature of this work is that the analyses are based only on observed streamflow data; no process-based models are used in this work. Process-based models require a large dataset for parameter calibration. Typically, the data include daily scale rainfall time series which contain measurement errors and spatial variability which is difficult to capture (Bardossy and Anwar, 2022, preprint). Also, there is structural uncertainty associated with process-based models (Beven and Smith, 2015). This is not to say that the process-based models are not useful for change detection, but that the analysis presented in this study can complement an analysis carried out using the process-based models.

In what follows, Section 2 describes the methodology used in this study. Section 3 describes the study area along with changes in a few climatic statistics across the USA. Section 4 describes the SSS across USA during the water years 1980-1989. In Section 4, a description of how different hydrologic processes may contribute to SSS is also provided. Section 5 discusses the changes in SSS. Sections 6 and 7 discuss the relationships of changes in SSS with the changes in climatic statistics and changes in watershed attributes. Section 8 concludes the paper.

2. Modeling Description

2.1 FARIMA model

The Fractionally differenced Auto-Regressive Integrated Moving Average (FARIMA; Montanari et al., 1997) model was used to capture the statistical properties of streamflow time series. FARIMA is a statistical time series model which is known to capture streamflow structure very well (Montanari et al., 1997 & 2000). The general form of the FARIMA model is

$$\Phi_p(B)(1-B)^d X_t = \Psi_q(B)\epsilon_t, \tag{1}$$

where X_t denotes streamflow at time-step t, B denotes the backward shift operator such that $BX_t = X_{t-1}$, d denotes a parameter of the model that takes a value between 0 and 0.5 for streamflow time series, and ϵ_t denotes uncorrelated white-noise. $\Phi_p(B)$ and $\Psi_q(B)$ denote p^{th} order autoregressive and q^{th} order moving average polynomials, respectively,

$$\Phi_p(B) = \sum_{i=0}^{p} \phi_i B^i\,,\ \phi_0 = 1, \tag{2}$$

$$\Psi_q(B) = \sum_{i=0}^{q} \psi_i B^i\,,\ \psi_0 = 1, \tag{3}$$

where ϕ_i and ψ_i are AR and MA parameters. Specifically, the terms AR1, AR2, … are reserved to refer to parameters ϕ_1, ϕ_2,…, respectively. Similarly, the terms MA1, MA2, … are reserved to refer to parameters ψ_1, ψ_2 ,…, respectively. When $d = 0$, the FARIMA model degenerates to an ARMA model. When d takes a positive integer value, it becomes classic ARIMA model promoted by Box & Jenkins (1970).

In the case of positive integer d values, the operator $(1-B)^d$ is the differencing operator as can be seen by setting $d = 1$: $(1-B)X_t = X_t - X_{t-1}$. Also, in this case, the process X_t is non-stationary. The interpretation of the model for the fractional d value is not intuitive. But its effect can be understood via the PSD of the process X_t. The PSD of the FARIMA model has the analytical form (Granger & Joyeux, 1980):

$$h(\omega) = |1-z|^{-2d} \frac{\left|\Psi_q(z)\right|^2}{\left|\Phi_p(z)\right|^2} \frac{\sigma_\epsilon^2}{2\pi}, \qquad z = \mathrm{e}^{-\iota\omega}, \tag{4}$$

where $|\cdot|$ denotes absolute value and $\iota = \sqrt{-1}$. For very small values of ω,

$$h(\omega) \propto \omega^{-2d}. \quad (5)$$

The PSD approaches ∞ as ω approaches 0. Also, Eq. (5) tells us that as d increases, $h(\omega)$ increases (Granger & Joyeux, 1980). In the time series domain, it means that an increase in the parameter d results in an increase in the amplitude of low-frequency (long timescales) fluctuations.

The effect of different parameters of the FARIMA model on time series characteristics has been illustrated in Figure 1 with generation of synthetic time series. In this illustration, the number of AR (p) and the number of MA parameters (q) were fixed to 1. The value of the MA parameter was fixed at 0.5; the values of AR parameter and d were varied. Figure1a shows the time series generated by setting FARIMA parameters to different values at a daily timescale. Figure 1b and 1c show the moving average of time series shown in Figure 1a with moving window lengths of 1 month and 1 year, respectively. When the value of d is increased from 0 to 0.25 keeping the AR1 parameter fixed, the two time-series show similar qualitative behavior at daily timescale (Figure 1a). But at the monthly and yearly timescales, the amplitudes of fluctuations are larger when $d = 0.25$. It shows that the parameter d affects the long timescale (low-frequency) behavior of the time series. The short timescale (high-frequency) behavior is unaffected by the parameter d. When the AR1 parameter is increased from 0.25 to 0.75 keeping the parameter d fixed, the amplitude of fluctuations becomes larger at all the timescales. Change in AR1 parameter has more profound impact on the daily timescale fluctuations than the change in parameter d. At long timescales, the change in parameter d has more profound impact on time series fluctuations than the change in AR1 parameter has.

Area under the PSD of a stationary process is equal to the variance of the process (Priestley, 1982). PSD divided by the variance is referred to as normalized power spectral density (NPSD). Also, the NPSD of a stationary process and its autocorrelation function form a Fourier transform pair (Priestley, 1982). Therefore, analyzing the NPSD of a stationary process is equivalent to analyzing its correlation structure. Also, NPSD provides a clean way of separating the contribution of different frequency components to the correlation structure. Therefore, in this study, the NPSD of the fitted FARIMA models was analyzed to detect SSS changes.

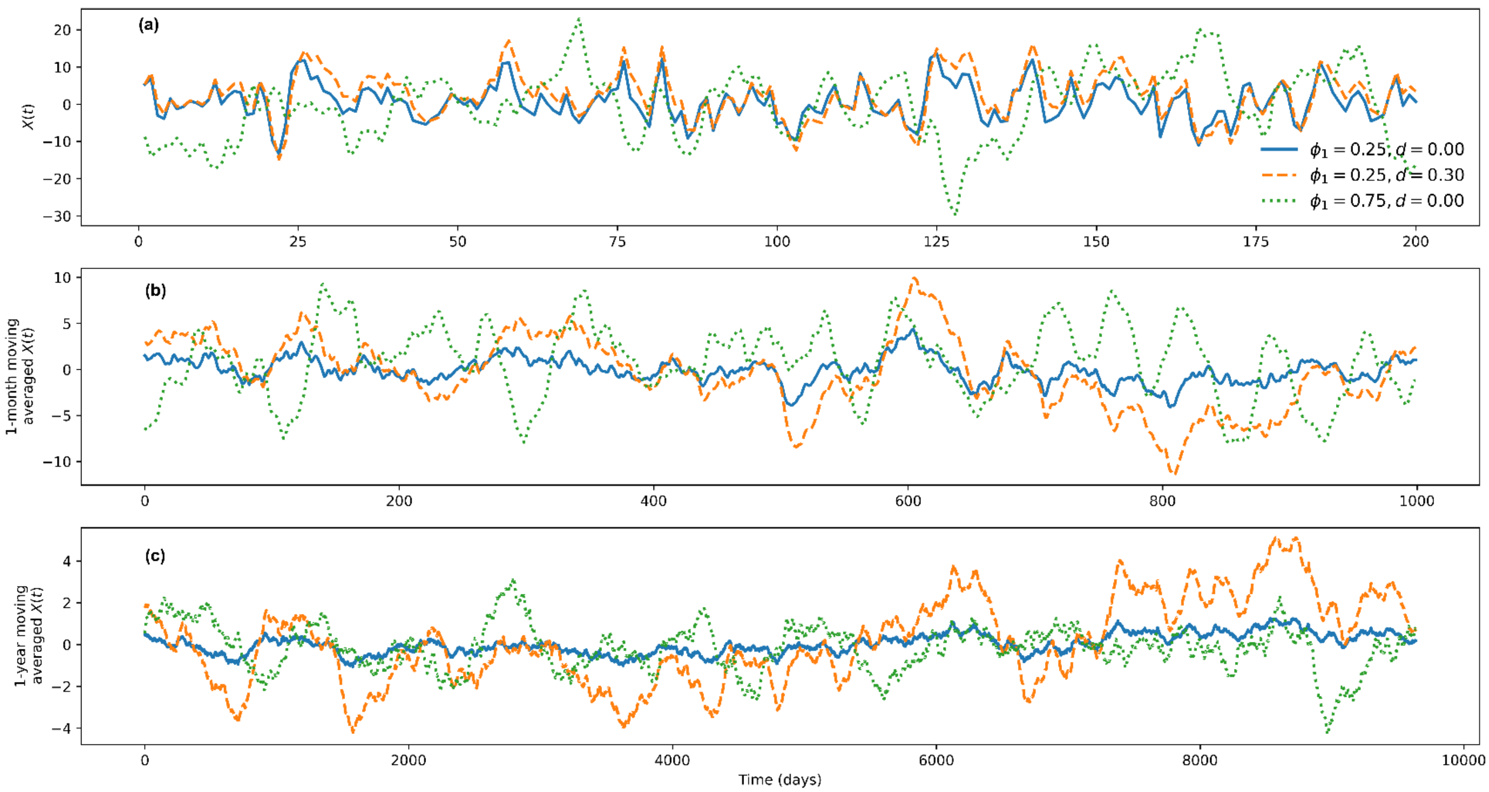

Figure 1. (a) Time series generated by FARIMA model for different value of AR1 parameter and d parameter at daily timescale; (b) 1-month and (c) 1-year moving average time series of time series shown in (a). Time series was generated for 10000 different timesteps. In subplots (a) and (b), first 200 and 1000 timesteps are shown, respectively, for the sake of clarity.

2.2 Parameter estimation of FARIMA models

Parameters of the FARIMA models were estimated using the same method as that of Monatanari et al. (1997). Details of the parameter estimation method have been provided in Supporting Information (SI, Text S1). Briefly, a two-step procedure was used to the estimate the parameters. In the first step, a preliminary estimate of the parameter d was obtained using two heuristic methods. The average of the two values obtained using these methods was considered as a preliminary estimate of d. Then the AR and MA model orders p_{opt} and q_{opt} were determined. In the second step, a statistical procedure (see SI, Text S1) was followed to estimate the parameter d, AR parameters, and MA parameters. In this step, the number of AR parameters were fixed to p_{opt} and q_{opt} as obtained in the previous step.

To validate the FARIMA models, the autocorrelations of the obtained residual time series were analyzed. The results are shown in SI (Text S2). For most of the models, the autocorrelations at any lag were statistically indistinguishable from zero. For a few models, however, the autocorrelation was greater than 0.15 at a few time-steps. These models and corresponding watersheds were removed from the subsequent analysis. The conditions imposed in this study is typically appropriate for model validation (see Montanari et al., 1997). The residuals, however, did not follow the Gaussian distribution for most of the models. But, as pointed out by Montanari et al. (1997) (and the references therein), deviation from Normality does not affect the parameter estimation of FARIMA models.

2.3 Measurement of change in power spectral density

To analyze the changes in SSS, a moving window approach was taken with the window length of 10 years and with moving step of 3 years (Table. 1). Thus, the study period (1980-2013 water years) was broken up into 9 overlapping windows of 10 years each. The FARIMA model was fit to deseasonalized time series for different moving average windows as illustrated in Table 1. Thus, as many sets of FARIMA parameters were obtained as the number of moving windows. Each set of parameters results in an NPSD ($f(\omega)$ vs. ω) computed by Equation (4). To detect the changes in SSS, the trend in area under $f(\omega)$ for different ranges of ω was computed (Figure 2). The frequency range was split into five different regions (units in cycles per day – c.p.d.): (1) less than $1/365$ c.p.d. (greater than 1-year timescales), (2) $1/365$ to $1/120$ c.p.d. (4-months to 1-year timescales), (3) $1/120$ to 1/30 c.p.d. (1-month to 4-months timescales), (4) $1/30$ to $1/15$ c.p.d. (2-weeks to 1-month timescales), and (5) greater than 1/15 c.p.d (less than 2-weeks timescale). For the ease of discussion, two more frequency regions were used: 1/365 to 1/30 c.p.d. (1-month to 1-year timescales) and greater than 1/30 c.p.d. (less than 1-month timescales). The area under NPSD in a given frequency region (ω_1, ω_2) is

$$F(\omega_1, \omega_2) = \int_{\omega_1}^{\omega_2} f(\omega)\, \mathrm{d}\omega, \tag{6}$$

which is equal to the contribution of the components with frequency between ω_1 and ω_2 to the total variance. Since the area under NPSD is equal to 1, an increase in the contribution of high-frequency contribution implies a decrease in low-frequency components as is also illustrated in Figure 2.

In what follows, area under NPSD in the frequency region greater than 1-year timescale will be denoted by F_0. Similarly, area under NPSD in the frequency region 4-months to 1-year timescales, 1-month to 4-months timescales, 2-weeks to 1-month timescales, less than 2-weeks timescales, 1-month to 1-year timescales, and less than 1-month timescales will be denoted by F_1, F_2, F_3, F_4, F_5, and F_6, respectively.

Let $F_i^j(\omega_i, \omega_{i+1})$ be the area under $f(\omega)$ for i^{th} frequency region and j^{th} time-window. The trend in $F_i^j(\omega_i, \omega_{i+1})$ across time periods can be estimated with a linear fit: $F_i^j(\omega_i, \omega_{i+1}) = \gamma j + c$, where γ is the trend, and c is the intercept. The sign of γ indicates whether the contribution of a frequency region to total streamflow variance is increasing (positive γ) or decreasing (negative γ) over time. The magnitude of γ indicates the extent of change: larger (smaller) magnitude of γ

implies larger (smaller) change. A trend was considered statistically significant if the p value of the slope γ was less than or equal to 0.05. We refer to this test as first significance test.

Table 1. An example of moving windows used for analysis.

Window Number	Time-period (years)
1	1980-1989
2	1983-1992
3	1986-1995
4	1989-1998
5	1992-2001
6	1995-2004
7	1998-2007
8	2001-2010
9	2004-2013

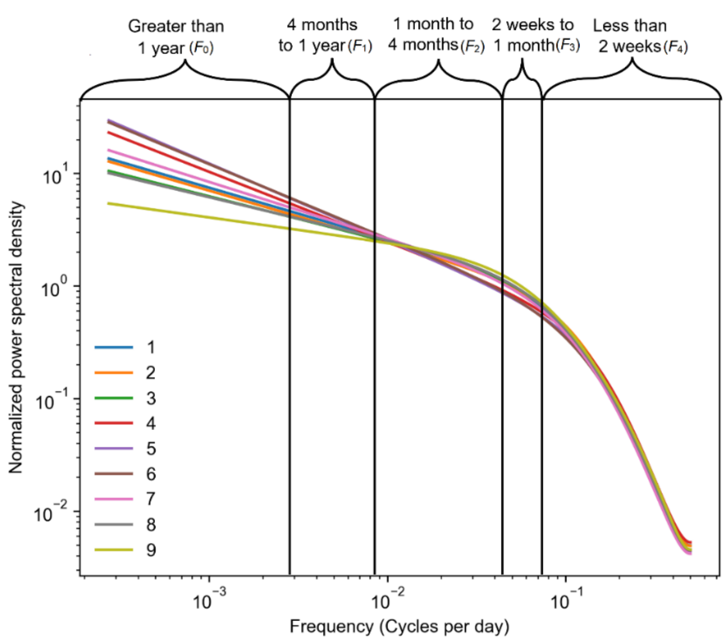

Figure 2. Normalized power spectral density over 9 different time-windows (see Table 1). The frequency range is divided into 5 different regions as indicated by the labels at the top of the plot.

In addition, statistical significance of each trend was computed by another method. Using the posterior probability distribution of the FARIMA parameters, the posterior probability distribution of NPSD was obtained. This, in turn, was used to compute probability distribution of the fraction of area under each frequency region of NPSD (see Figure 2 for frequency regions) for all the time windows. Thus, for each frequency region, we had probability distribution of $F_i^j(\omega_i, \omega_{i+1})$ for the first and last time-windows. Let these probability distributions be denoted by $P_1(F)$ and $P_2(F)$ with respective mean values m_1 and m_2. For the trend to be significant, we imposed the condition that m_1 and m_2 should belong to different statistical populations. Toward this end, a probability p_s was computed:

$$p_s = \begin{cases} \dfrac{P_1(F \geq m_2) + P_2(F \leq m_1)}{2}, & m_1 < m_2; \\ \dfrac{P_1(F \leq m_2) + P_2(F \geq m_1)}{2}, & m_1 \geq m_2. \end{cases} \tag{7}$$

For the trend to be significant, p_s should be less than 0.05. We refer to this test as the second significance test. In summary, a trend was deemed statistically significant only if it came out to be significant using both first and second statistical significance tests. This means that the change in SSS should be consistent in time and the SSS in the first and last time-windows should be significantly different.

The first and second significance tests collectively ensure that the changes in regime are robust. If change in regime in a watershed is significant according to first significant test, it is still possible that first and last time-windows have similar regimes. Such a change is unlikely to be robust; the second significance test helps us identify and discard such cases. Changes in regime were gradual in some watersheds and sudden in other watersheds. Therefore, the Mann-Kendall test could not be reliably applied to many of these watersheds. For the sake of completeness, we still applied the Mann-Kendall trend test. We found that of all the watersheds for which changes in SSS were statistically significant according to first and second significance tests, 70% of the watersheds had statistically significant changes according to Mann-Kendall test also. For the majority of the 30% watersheds for which Mann-Kendall test concluded that changes were statistically insignificant, the changes were abrupt.

Figure 3 illustrates the problem in using Mann-Kendall test. It shows the boxplots of F_4 values for nine time-windows for a watershed. The change in F_4 is statistically significant according to first and second significance test, but the change is statistically insignificant according to Mann-Kendall test. It is clear from Figure 3 that the F_4 values in last six time-windows are very different from those in first three time-widows. The Mann-Kendall test recognizes this as a statistically insignificant change because there are fluctuations in values of F_4 within last six window. But this fluctuation is smaller than the change in F_4 as one moves from window 3 to window 4.

It is also clear from Figure 3 that length of time-window (3650 days in this study) does not have any effect over the conclusion that the value of F_4 has changed significantly. Even if we had compared the NPSD computed by using first and last 15 years of daily streamflow, the conclusion would have been that the F_4 values have changed. This was true of other watersheds also where first and second significance test concluded that the F_4 values have changed. Further, we repeated the analysis using a 15-year time-window to test the robustness of the results against the length of the time-window; the results presented in the paper were unaffected by changing the time-window length to 15 years. For completeness, some more plots illustrating the changes in SSS are shown in SI (Text S5, Figures S13, S14, & S15); these plots also illustrate the robustness of the changes in SSS reported in this study.

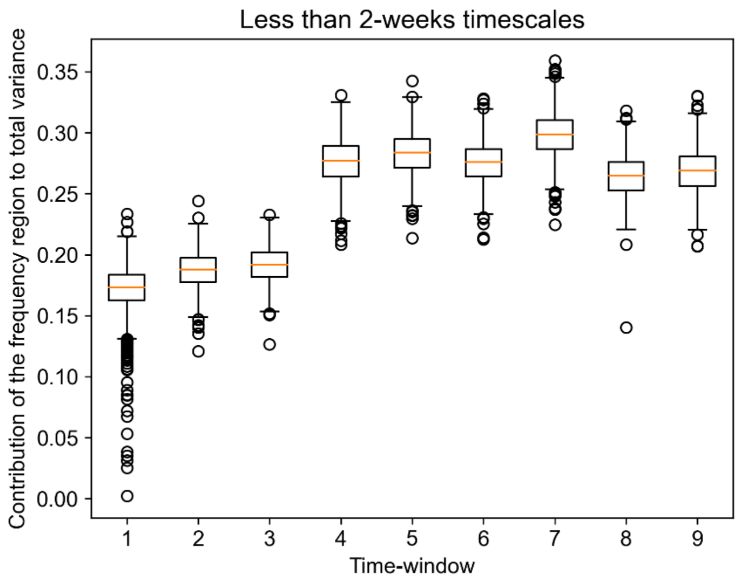

Figure 3. Illustration of change in < 2-weeks timescales component (F_4) for a watershed. In this case, the change is statistically significant according to first and second significance test, but statistically insignificant according to Mann-Kendall test. It is clear that the values of F_4 for last 6 time-windows are significantly different from those in the first three time-windows. The lower and upper whiskers represent $Q_1 - 1.5 * IQR$ and $Q_3 + 1.5 * IQR$, respectively. Here Q_1 and Q_3 denote 25th and 75th percentiles represented by lower and upper edges of the boxes, and IQR denotes inter-quartile range, that is, $Q_3 - Q_1$.

We note that Gudmundsson et al. (2011) studied the contribution of low-frequency components (greater than 1-year timescale) to total streamflow variance in several European watersheds. They estimated this quantity by using the LOWESS method (Cleveland, 1979) directly instead of using spectral decomposition as discussed above. They did compare their results with those obtained by using the spectral method and concluded that both the methods yield similar estimates. But they only studied the spatial variation of this quantity, not the change in time.

2.4 Different geographical regions of the USA, rain- and snow-dominated watersheds

For the sake of discussion, reference to different geographical regions of the USA will be made. The spatial extent of these regions is shown in Figure A1 (Appendix A). The rain-dominated watershed are the ones located in the Pacific region (except Sierra Nevada), the Gulf Coast, the central and the southern Great Plains, the central and the southern Mississippi Valley, and one watershed in the Atlantic Coast. Snow-dominated watersheds are the ones located in the Sierra-

Nevada, the Rocky Mountains, the High Plains, the northern Great Plains, and the Great Lakes region. A few watersheds in the Pacific Northwest were also snow-dominated. The watersheds located in the northern Mississippi Valley could not be classified as either snow- or rain-dominated.

2.5 Methodology for relating changes in statistical structure of streamflows with climatic statistics, and watershed attributes

To understand the changes in SSSs, statistical methods were used. First, the variables related to the change in $F_i, i = 0,1, \ldots 6$ were identified. Second, possible mechanisms via which each variable might have affected the F_i values were hypothesized. Watersheds were divided into two groups: snow-dominated and rain-dominated watersheds. The analysis was carried out separately for these two groups. Note that many of the snow-dominated watersheds also experience rain (and vice-versa) but the SSS is significantly controlled by snow. Further, the only difference between the analyses of snow- and rain-dominated watersheds is that for snow-dominated (rain-dominated) watersheds some predictor variables exclusive to snow-dominated (rain-dominated) watersheds were derived; other predictor variables were identical for all the watersheds. The locations of snow- and rain-dominated watersheds used are shown in Figures S11 and S12, respectively.

The variables explored include static catchment attributes including soil properties, geological properties, topography, and climate. Change in climatic statistics were also explored as possible causes of change in F_is. These include variables related to change in precipitation and change in temperature. For example, change in total annual precipitation depth, change in OND (Oct-Nov-Dec) total precipitation depth, and change in mean annual temperature. Changes in climatic variables were computed using the same moving windows as for the case of change in SSS (Table 1). Additionally, variables capturing snowmelt dynamics in snow-dominated watersheds and rainfall-runoff dynamics in rain-dominated watersheds were also used. The details of these variables are given in Sections 6 and 7 and in SI (Texts S3 and S4). A list of all the variables used in this study is included in Table A1.

Variables important for explaining the change in F_i were identified using the random forest algorithm (Brieman, 2002) and simple linear regression. Random forest has the advantage that it can identify non-linear relationships between two variables. However, we found that both the random forest and linear regression yielded the same variables as important. A variable was considered important using simple linear regression if the regression coefficient was significantly different from 0 at a 5% significance level. Two linear fits were made for each combination of ΔF_i and predictor variable: (1) using all the watersheds, and (2) using only the watershed for which ΔF_i was significant according to both first and second significance test. All the variables for which the slope of either of the two linear fits was significant at the 5% significance level were considered important.

We found that even though linear regression and random forest could identify the important predictor variables, there was large scatter in the relationship between ΔF_i with other predictor variables. Essentially, the linear fit may have a statistically significant slope, but it is possible that not all the watersheds satisfy the relationship suggested by the line (similar argument applies to random forest algorithm). Therefore, probability densities of important variables conditioned upon the event that ΔF_i was positive or negative were plotted to understand the effect of a variable on ΔF_i. This procedure is similar to computing mutual information between ΔF_i and a variable, but more transparent as shown below. The aim of this analysis is to identify what characteristics of a watershed are related to positive or negative changes in F_i. For example, we observed that arid and humid watersheds exhibited different kinds of changes in SSS.

Note that random forest and linear regression are merely used to identify the important variables. The conclusion drawn in this study are based upon the differences in probability distributions of important variables conditioned upon positive and negative changes.

3. Study area and data

To achieve the objectives of this study, Catchments Attributes and Meteorology for Large Sample studies (CAMELS) dataset (Addor et al., 2017a & 2017b) was used. The CAMELS dataset was chosen because it contains hydro-meteorological dataset for a large number of watersheds (671) across the contiguous USA. Also, the CAMELS watersheds are unregulated and free of the anthropogenic land-use changes such as deforestation. The time-period of the data is water years 1980-2013. In this study, we included watersheds that had at least 30 years of complete data; there were a total of 614 such watersheds.

Exploratory analysis shows that significant warming has occurred in CAMELS watersheds across USA. Figure 4 shows the trends in several climatic variables over the study period. These trends were computed as slope of the linear fit on the plot of climatic variable vs. time-window. A trend was considered statistically significant if the p value of the slope was less than 0.05. The same time-windows were used for the computations of these trends as shown in Table 1. Figure 4 discusses the following variables: mean minimum daily temperature (average of the minimum daily temperature over a time-window), mean maximum daily temperature, OND mean maximum daily temperature (average of Oct-Nov-Dec maximum daily temperature over a time-window), AMJ (Apr-May-Jun) mean maximum daily temperature, number of rain days (number of days when rain occurred in a decade), number of storms (number of rainfall event where an event consists consecutive non-zero rainfall days), mean storm depth (average rainfall over non-zero rainfall days), and total rainfall depth (total rainfall within a decade).

Mean minimum daily temperature has increased (positive trend) for most of the watersheds with largest increases across the western US. There exists considerable variation in the trends of mean maximum daily temperatures. The snow-dominated watersheds located in the Rocky Mountains and the High Plains have experienced a large increase in mean maximum daily temperatures. Several rain-dominated watersheds located in the Pacific Northwest and the Pacific Coast have experienced a negative trend in mean maximum daily temperatures. Many of the watersheds located in the eastern USA experienced a negative trend in mean maximum daily temperatures (though statistically insignificant), especially those in the Great Plains. Further, Figures 4c and 4d show trend in OND (Oct-Nov-Dec) and AMJ (April-May-Jun) maximum daily temperature. Maximum daily temperatures in OND months increased across USA with large increases in the Great Plains, the High Plains, the Mississippi Valley, the Atlantic Coast, and the Great Lakes region. The OND maximum daily temperature trends are moderate in the Gulf, the Pacific Coast, and the Pacific Northwestern watersheds. Maximum daily temperature in AMJ months has decreased across USA except in the western Gulf Coast. The most significant decreases were noted in the Pacific Northwest, the Pacific Coast, and the Atlantic Coast. As will be discussed below, changes in OND and AMJ maximum temperatures appears to have significant control over changes in the SSS.

Figures 4e-4h shows changes in rainfall statistics. There is a strong north-south gradient in the trends in the number of rain days: In northern (southern) watersheds, the number of rain days have increased (decreased). The trends in the number of storms have a weak north-south gradient. In many regions, the number of rainstorms has decreased but the number of rain days have increased. This implies that more rain is falling in fewer storms of longer duration in these regions. These regions include the Pacific Northwest and the north-eastern part of Atlantic Coast. In the north-eastern part of Atlantic coast, the total rainfall depth and the mean storm depth – the average rainfall depth on rainy days – has increased. The trends in the total rainfall depth have a strong north-south gradient, especially in the eastern USA: total rainfall increased in the northern watersheds and decreased in the southern watersheds. The mean storm depth has more spatial variability compared to the other three rainfall statistics. The only clear patterns are that the mean storm depth has increased in the Atlantic Coast region and decreased in the High Plains region.

In summary, Figure 4 convincingly shows that both the temperature and rainfall statistics have changed across the USA. Since temperature and precipitation both have strong control over SSS, at least some of the CAMELS watersheds are likely to have undergone a SSS change. Increase in atmospheric CO_2 can also result in changes in vegetation characteristics such as water use efficiency (Donohue et al., 2013) which, in turn, may affect the SSS. Significant increases in temperatures along with the fact that global average CO_2 has increased over the period 1980 to 2014 (from 339 ppm in 1980 to 397 ppm in 2014; Dlugokencky & Tans, gml.noaa.gov/ccgg/trends/, accessed on 17 Mar 2022) indicates significant change in climate has occurred between this period beyond the natural climate variability.

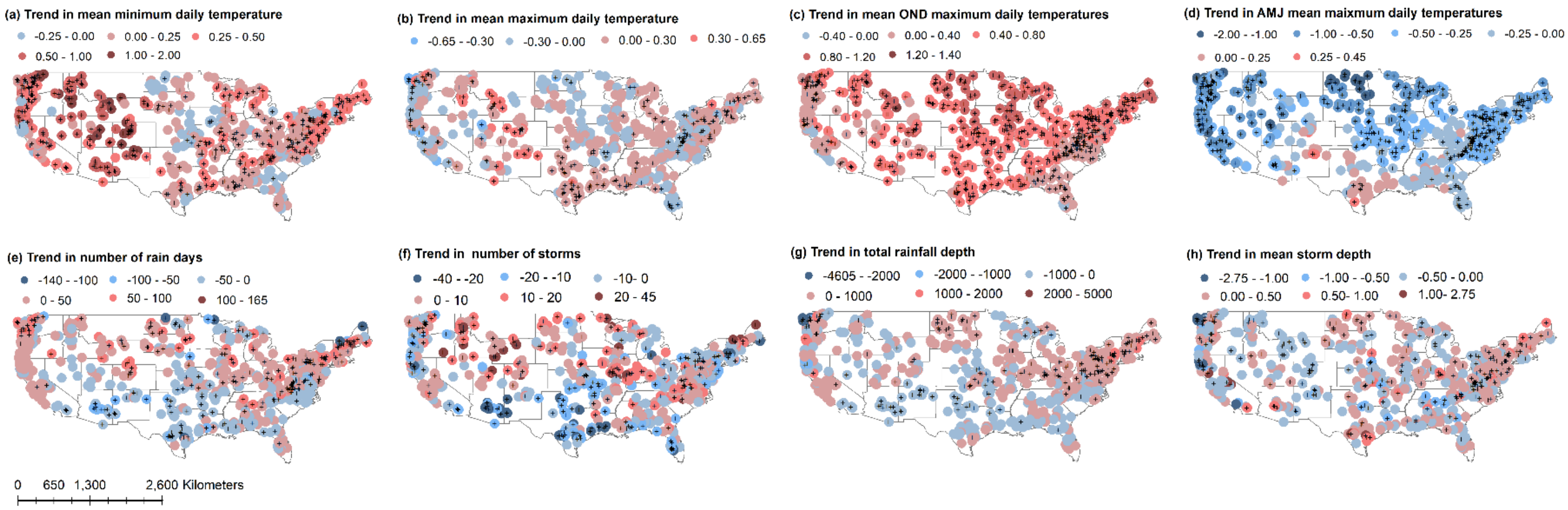

Figure 4. Trends in climatic variables (a) daily minimum temperature, (b) daily maximum temperature, (c) and (d) OND (Oct-Nov-Dec) and AMJ (Apr-May-Jun) daily maximum temperatures, respectively, (e) number of rain days (in days decade^{-1}), (f) number of storms (in decade^{-1}), (g) total rainfall depth (in mm decade^{-1}), and (h) mean storm depth (in mm day^{-1} decade^{-1}). The units of all the temperature statistics are °C decade^{-1}. The red colored symbols indicate positive trend and blue colored symbols indicate negative trend. The '+' sign indicates that trend is statistically significant at 5% level, and the trend is computed as the slope of linear trend line A storm refers to a rainfall event consisting of non-zero rainfall on consecutive days.

4. Spatial distribution of streamflow statistical structure (SSS) in the USA

Figure 5 (a, b, c, d) shows the contribution of different frequency regions to streamflow variance in CAMELS watersheds during the first time-window (1980-1989 water years). The aim of this section is to understand the spatial variability of SSS across the USA which would put the changes in SSS in proper context. As in the preceding discussion, reference to different geographical regions of the USA will be made in this discussion (See Figure A1 in Appendix A).

The contribution of greater than 1-year timescales components to total streamflow variance (F_0) was less than 10% in most of the rain-dominated watersheds of the eastern USA and the Pacific Northwest (Figure 5c). Conversely, large contributions from this frequency region were found in some snow-dominated watersheds in the Rocky Mountains region, the High Plains, the Sierra Mountains in California, and the Pacific Coast.

The contribution of the 1-month to 1-year timescale component (F_5; Figure 5b) was very small in the Great Plains and the Mississippi Valley compared to that in other regions. The highest value of F_5 (>50%) was found in the snow-dominated watersheds of the Rocky Mountains and the High Plains. In the Pacific Northwest and the Atlantic Coastal region, F_5 values range from 25 to 50%. The values of F_5 follow the broadscale pattern of the baseflow index (BFI; see Figure 4 in Addor et al., 2017). The BFI values are below 0.5 in the Great Plains and the Mississippi Valley, greater than 0.6 in the Rocky Mountains and the High Plains, and between 0.40 and 0.60 in the Pacific Northwest and the Atlantic Coastal region. Moreover, the scatter plot (not shown) of the BFI and F_5 shows that as the BFI increases from 0 to 0.4, F_5 value also increases. Beyond, a BFI value of 0.4, however, there exist a few watersheds where F_5 values are low. Overall, the contribution of baseflow to total streamflow appears to be an important factor in determining the values of F_5. Interflow might also contribute to the 1-month to 1-year frequency region.

The contribution of less than 1-month timescales component to total streamflow variance (F_6) is small (<25%) in the cold snow-dominated watersheds of the western USA (Figure 5a). In the Pacific Northwest and the Pacific Coast, F_6 values are between 25% and 75%, but mostly greater than 50%. In most of the eastern USA watersheds, the contribution of this frequency component is greater than 50%. In the Great Plains and the Mississippi valley, the contribution of this component is greater than 75% in many watersheds. These are dry watersheds where most of the rainwater evaporates back into the atmosphere, and only intense storms reach the river network. Therefore, the contribution of low (high) frequency components is very low (high) in these watersheds. Since the contributions of low- and high-frequency components are one-to-one related (an increase in one implies a decrease in the other), BFI explains some of the spatial variations in F_6: lower BFI means higher F_6. It is noteworthy that in the snow-dominated watersheds with the fraction of snow > 0.40 (fraction of precipitation falling as snow), the value of F_6 increases with an increase in mean rainfall.

In the rain-driven watersheds, a linear relationship between the slope of the flow duration curve (FDC; Addor et al., 2017) and F_6 was found (slope $= -0.054$, p-value $= 0.0045, R^2 = 0.033$). Smaller slopes of FDC imply smaller variability in streamflow. Thus, the negative correlation between FDC slope and the contribution of the high-frequency region indicates that watersheds with less variation in streamflow values exhibit more contributions from the high-frequency components. For example, in ephemeral streams, streamflow variation is low as it stays dry during most of the water year; therefore, the low (high) frequency component is very small (large).

The contribution of the 2-weeks to 1-month timescale component to total streamflow variance (F_3) is very small for most of the watersheds (Figure 5d). But there exists a cluster of watersheds in the Pacific Northwest where F_3 values are greater than 20%. In fact, in most of the Pacific Northwestern watersheds, F_3 values are greater than 15%. The F_3 values are also greater than 15% in the several eastern snow-dominated watersheds.

It was observed that F_3 was positively correlated with mean precipitation ($R^2 = 0.206$, p-value $= 1.70 \times 10^{-28}$), and negatively correlated with potential evapotranspiration (PET; $R^2 = 0.115$, p-value $= 1.62 \times 10^{-15}$). This indicates that F_3 values are high in watersheds with high total precipitation and low ET which are likely to be humid watersheds. Further, F_3 was negatively correlated with low rainfall frequency ($R^2 = 0.157$, p-value $= 6.15 \times 10^{-21}$) and, also, negatively correlated with high rainfall frequency ($R^2 = 0.093$, p-value $= 1.25 \times 10^{-12}$). Here, high- and low-frequency rainfall in a watershed is equal to the fraction of days rainfall is greater than 5 times the mean rainfall and less than 1 mm, respectively. It indicates that in watersheds where rainfall event characteristics are such that it allows the water to stay in the soils for a long time compared to the timescale of quick flow and percolation, the F_3 values are high. These results indicate that interflow may be responsible for creating the 2-weeks to 1-month timescales component. Wu et al., (2021) showed that lateral preferential flow is an important streamflow generation mechanism in Pacific Northwestern watersheds.

Figure 5e shows the spatial variation of the parameter d in CAMELS watersheds. There is a large spatial variation in the values of d, but some general patterns can be observed. The very high values of d (>0.30) are typically observed in western snow-dominated watersheds where the contribution of low-frequency components was significant. In most of the eastern rain-driven watersheds, the d values were less than 0.30. There was a strong linear relationship between BFI and d value (slope $= 0.22$, $p \approx 10^{-31}$, $R^2 = 0.23$). Also, the linear relationship was stronger when BFI increased from 0 to 0.25 - at very low values of BFI the d values were close to 0. This indicates that the baseflow is the essential factor for the existence of long-term persistence in streamflow time series. Many of the watersheds in the Pacific Northwest, the Great Plains, the Great Lakes, and the Atlantic Coast region had d values less than 0.10, despite having moderately high values of BFI (>0.40) except in the Great Plains. The reason for such small values of d is not clear and further exploration is out of the scope of this paper.

The long-term persistence (high d value) in a time series may result from an aggregation of short-memory processes (Granger, 1980). Muldesee (2007) argued that long-term persistence in streamflow time series may also be a result of the aggregation of several short-memory processes in a watershed. They showed that the value of d increases with increasing drainage area as one moves downstream in a river network. Therefore, it is reasonable to expect that watersheds with large drainage areas may show higher d value in their corresponding streamflow time series. Such a relation between drainage area and d, however, was not observed in this study.

It can be concluded that long-timescale fluctuations and long-term persistence even in a deseasonalized streamflow time series are determined by low-frequency processes such as the contribution of baseflow, the fraction of snow, and possibly interflow. High-frequency components are determined by quick flow, interflow, and ET. Also, note that other researchers have reported higher contributions of the low-frequency components to streamflow (e.g., Gudmundsson et al., 2011) compared to those reported in this study. This is due to the seasonal component of the hydrologic cycle. In our study, the seasonal component had been removed from the streamflow time series; therefore, F_0 values came out to be smaller.

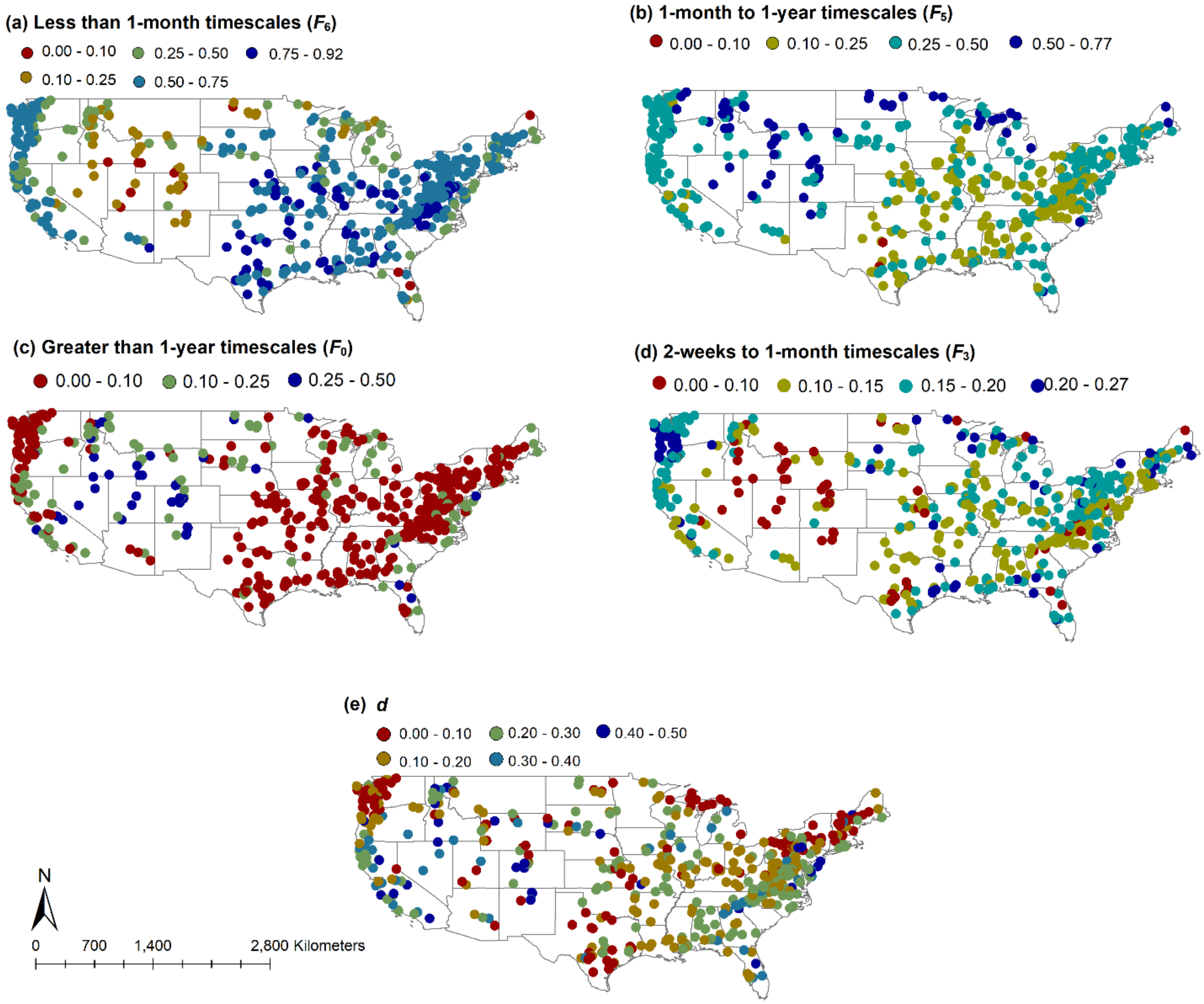

Figure 5. (a), (b), (c), (d)Area under NPSD in different frequency regions, and (e) value of the parameters d across USA. These results correspond to first 10-year moving window.

5. Change in streamflow statistical structure (SSS) as measured by change in NPSD

Figure 6 shows the spatial distribution of trends in $F(\omega_i, \omega_{i+1})$ for short timescales: Less than 1-month (F_6), 2-weeks to 1-month timescales (F_3), and less than 2-weeks (F_4). Overall, the spatial distribution of trends is patchy. But a spatial structure, albeit weak, is still visible such that watersheds with positive (negative) changes tend to be clustered together in small groups. This is especially true for the watersheds located in the Pacific Northwest, the Gulf coast, the Atlantic coast, and the Great Lakes region (See Figure A1 in Appendix A for a reference to these geographical regions). It indicates that the process(es) that has caused these changes is spatially correlated: change in climate seems to be one of the causes. But climate change alone cannot explain these changes since the correlation length of these trends is significantly smaller than the correlation length of trends in climatic variables such as temperature and rainfall (Figure 4). Further, it implies that the effect of climate change on the SSS is strongly modulated by watershed characteristics such as soil properties, and geomorphological characteristics. This will be explored in subsequent sections.

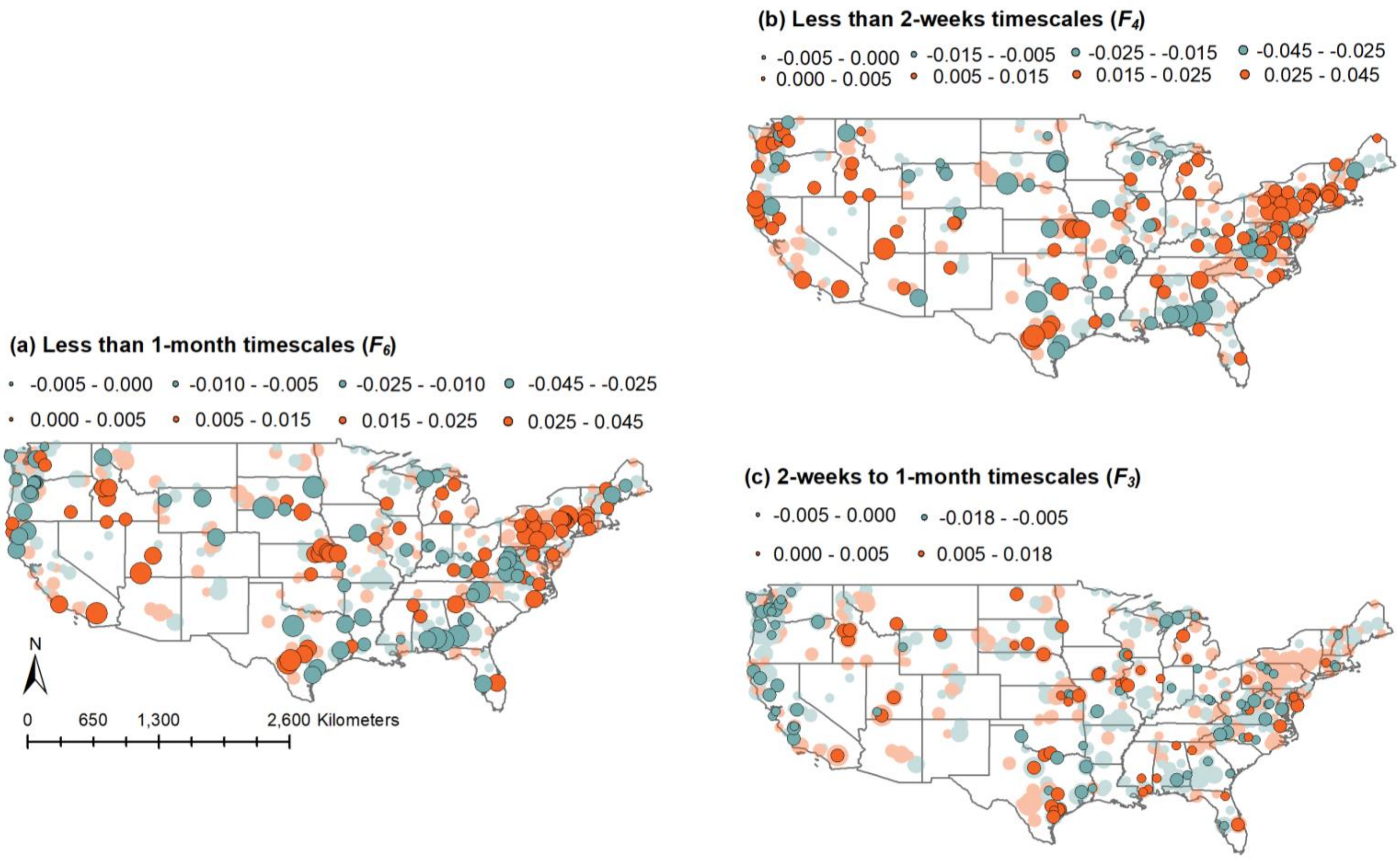

Figure 6. Trend in area under NPSD for high-frequency regions (a) less than 1-month timescale, (b) less than 2-weaks timescale, and (c) 2-weeks to 1-month timescale. The watersheds with transparent symbols indicate that the trend is statistically insignificant according to the first significance test. Larger (smaller) sized circles represent larger (smaller) magnitude of change.

Most of the snow-dominated watersheds in the eastern USA (located in the northern Atlantic Coastal region and the state of Michigan) exhibited positive trends in F_6 and F_4. In the western snow-dominated watersheds, both negative and positive trends in F_6 and F_4 were observed but most of the statistically significant trends were positive. Watersheds with negative trends were mostly located in the High Plains. The trends in F_3 were positive in most of the Rocky Mountain watersheds and negative in the eastern snow-dominated watersheds, but the magnitude of the trend was very small compared to that in F_4. Overall, it can be concluded that the contribution of high-frequency components to total variance has increased over the study period in the majority of the snow-dominated watersheds, with the exception of the High Plains. Several different mechanisms are plausible that could affect this change: (1) An increase in runoff-producing rainfall events, (2) a change in temperature snow relationship (Horner et al., 2020), (3) a change in snow storage (including spatial distribution), and (4) a change in temperature regime. It is likely that the combination of these mechanisms rather than one individual mechanism is responsible for the changes.

In the rain-driven watersheds, other than spatial clustering of positive trends with positive trends and that of negative trends with negative trends, a few other patterns are visible. Most of the humid watersheds located in the Pacific Northwest region and the Gulf Coast region showed a negative trend in F_6. But the trend in F_4 was positive in many of the watersheds in the Pacific Northwest, while in the Gulf Coast the trend in F_4 was also negative. Overall, it appears that humid watersheds are becoming drier which is possible due to the changes in rainfall statistics in these watersheds. Another possibility is that the change in evapotranspiration statistics in these watersheds is caused by the change in temperature which, in turn, will change the soil moisture dynamics. A decrease in mean soil moisture in humid watersheds will result in a decrease in the contribution of high-frequency components to streamflow. This will be discussed in subsequent sections. In the Great Plains, both increasing and decreasing trends in F_4 and F_6 were observed.

The trends in F_3 showed two clear patterns: (1) Most of the statistically significant trends were negative in the watersheds located in the Pacific and the Atlantic Coastal regions, and (2) Most of the statistically significant trends in the Rocky Mountains, the Great Plains, the Mississippi Valley, and the Gulf Coast were positive. The trends in F_3 were of small magnitude compared to those in F_4 and F_5. This is because the contribution of F_3 (one month to one-year time scales) is very small in most of the watersheds, to begin with. A remarkable result is that the F_3 values have decreased in almost all the Pacific region watersheds. Since the F_3 values were very small in all the watersheds across the USA, the changes in F_3 were expected to be highly variable in space. Therefore, the presence of only negative changes in the F_3 values in the Pacific region watersheds indicates a significant, systematic, and common causal mechanism.

Figure 7 shows the spatial distribution of the trends in long timescale fluctuations: Greater than 1-year (F_0), 4-months to 1-year (F_1), and 1-month to 4-months (F_2) timescales. Similar to short-timescale trends, a weak spatial clustering of positive trends with positive trends and negative trends with negative trends are observed for long timescale trends. The magnitude of the trends in F_0 is larger in the watersheds located in the western USA. In most of the western snow-dominated watersheds, the value of F_0 decreased, and the magnitudes of decrease are relatively large. But the trend was statistically significant only in three watersheds, which might be due to the small magnitude of F_0 value. There is some spatial variability in the F_0 in the eastern USA snow-dominated watersheds. This is explained by the fact that in the eastern snow-dominated watersheds, the contribution of components at greater than 1-year timescales is smaller.

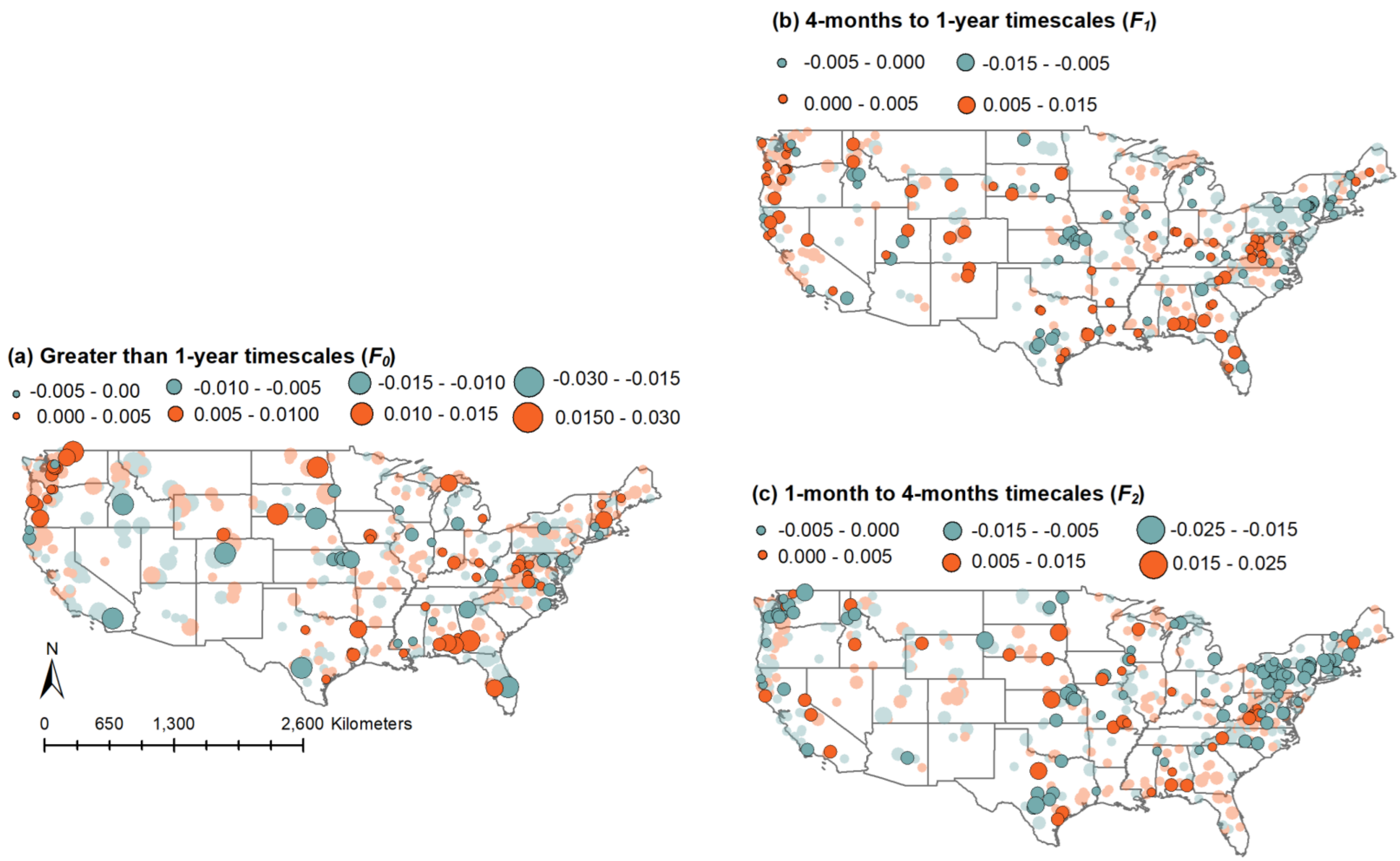

Figure 7. Trend in area under NPSD for low-frequency regions (a) greater than 1-year timescale, (b) 4-months to 1-year timescale, and (c) less than 4-months timescale. The watersheds with transparent symbols indicate that the trend is statistically insignificant according to the first significance test. Larger (smaller) sized circles represent larger (smaller) magnitude of change.

The values of F_1 and F_2 decreased in most of the eastern snow-dominated watersheds. The value of F_1 increased in all the snow-dominated watersheds in the High Plains while it decreased in many of the Rocky Mountains. The plausible reasons for the difference in trends of the eastern and the western snow-dominated watersheds are discussed below.

Most of the rain-dominated watersheds in the Pacific Northwest exhibited positive trends in F_0 and F_1, and negative trends in F_2. Similarly, most of the watersheds in the Pacific Coast exhibited negative trends in F_0 though trend was statistically significant only for one watershed. The trends in F_0, F_1, and F_2 were positive in most of the Gulf Coast watersheds. Most of the rain-dominated watersheds in the Great Plains exhibited a decrease in F_0, F_1, and F_2. But there were several watersheds in this region where F_0, F_1, and F_2 increased.

In summary, SSS has changed in many of the watersheds across the USA. There is some spatial structure in the regime change: watersheds close to each other show similar types of changes. The spatial structure of change in snow-dominated watersheds is stronger than in rain-dominated watersheds. Also, the western and the eastern snow-dominated watersheds showed some differences in trends in long timescale components. In the western watersheds, the negative trends were observed in F_0 values. In the eastern watersheds, negative trends were observed in F_1 and F_2. Also, positive trends in F_1 were observed in the western snow-dominated watersheds. In the humid watersheds of the Pacific Northwest and the Gulf Coast, the contribution of high-frequency components decreased. The next two sections focus on the causes of regime change in snow and rain-dominated watersheds, respectively. The discussion of causes of change in the high-frequency and the low-frequency components is generally limited to the F_6 and F_5, respectively.

6. Causes of SSS change in the snow-dominated watersheds

In this section, we explore the causes of SSS changes in snow-dominated watersheds. Most of these watersheds are in the Sierra Nevada in state of California, the Rocky Mountains, the High Plains, the northern Great Plains, and the Atlantic region. A few watersheds are also located in the Pacific Coast (See Figure S11 in SI). There are other watersheds where snowmelt contributes to streamflow, but rainfall is the primary driver in those watersheds. In snow-dominated watersheds, snowmelt is the primary driver of streamflow. Snow accumulates during the winter season during low temperatures and melts during spring and early summer due to rising temperatures. The process of snowmelt is largely controlled by the amount and spatial distribution of snowpack, measured as snow water equivalent (SWE), and dynamics of temperature. The changes in SSS in snow-dominated watersheds may occur due to change in the SWE and/or temperature dynamics. Change in either of the two will result in the change in temperature-snowmelt relationship. Note that precipitation falls as liquid also in these watersheds but that is the secondary determinant of SSS.

In this study, snow signatures proposed by Horner et al. (2020) were used to identify the changes in temperature snow relationship. They defined streamflow, temperature, and SWE regimes as a 30-day moving average of their respective seasonal components. Let us denote streamflow, temperature, and SWE regimes by Q_{reg}, T_{reg}, and SWE_{reg}, respectively. Figure 8 shows the relationship between temperature and streamflow regimes for a hypothetical snow-dominated watershed. The segment AB is the snowmelt period where both streamflow and temperature rise. Streamflow reaches its peak at point B. After point B, temperature continues to rise but streamflow decreases because of the lack of snow availability. During segment CD, temperature decreases without significant change in streamflow. During the segment DA, snow accumulates. The segments AB and CD capture the snowmelt dynamics. In this study, the slope and intercept of the lines AB, denoted by δ_{snow} and β_{snow} were used as snow signatures. The rationale for using these two qualities has been further described in SI (Text S3). The slope, δ_{snow}, is a measure of rate of increase of snowmelt per unit increase in temperature. The intercept β_{snow} is the streamflow when the mean temperature is zero and snowmelt has not started. The trends in these snow signatures are discussed in SI (Text S3, Figure S11). In the context of this paper, trends in snow signature are related to the change in snowmelt dynamics.

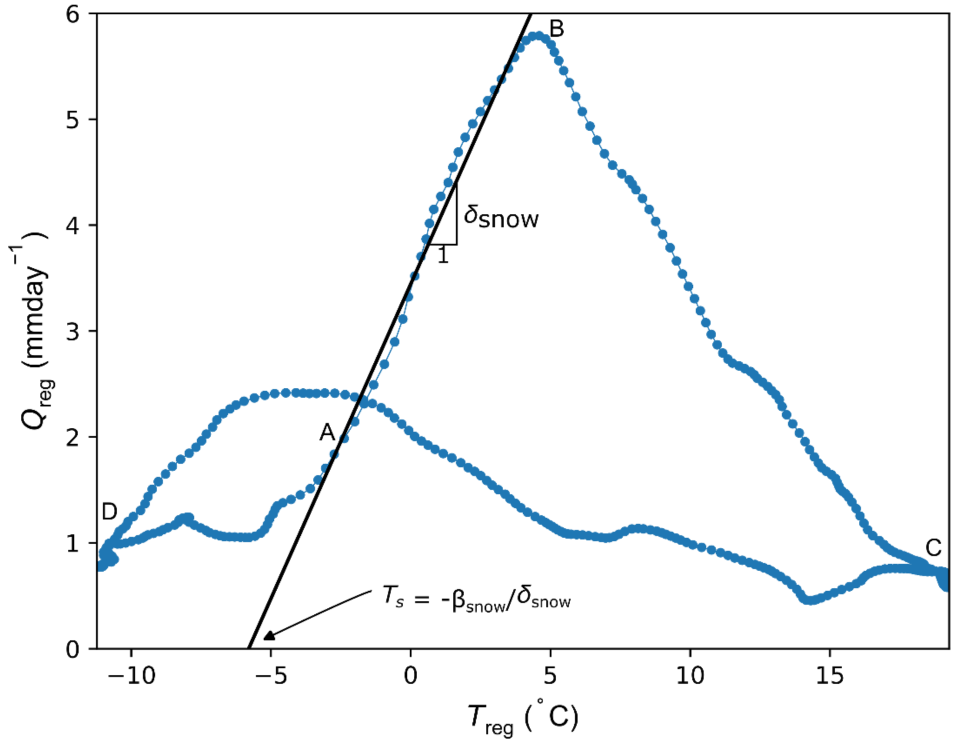

Figure 8. Relation between the temperature and streamflow regimes. T_{reg} is the temperature regime of the mean watershed temperature. T_s denotes the threshold mean watershed temperature at which snowmelt starts. The locations of the points A, B, C, and D is approximate. The direction of plot is A → B → C → A.

Next, we look at how the change in snowmelt dynamics along with other watershed properties have affected the SSS. Figure 9 shows the important predictor variables that determine the change in F_6 . Blue and orange solid curves are the probability densities of variables conditioned upon the positive and negative trends for all the watersheds, respectively. Green and red dash curves are the probability densities of variables conditioned upon the positive and negative trend for all the watersheds where the trend was statistically significant.

Several important variables were related to the change in the rainfall statistics: the trend in mean storm depth, the trend in JAS (July-August-September) average rainfall depth, the trends in average high rainfall duration and depth, and the trend in total storm depth. An increase in all these statistics is associated with an increase in F_6. For example, in watersheds where mean storm depth increased, positive changes in F_6 were more likely. This is expected because an increase in all of these four variables would increase high-frequency fluctuations in streamflow. The mean storm depth increased in most of the eastern snow-dominated watersheds (Figure 4). It tells us that increase in F_6 in the eastern snow-dominated watersheds might be related to an increase in precipitation.

Mean watershed temperature is another important variable: Watersheds with warmer temperatures were more likely to exhibit an increase F_6. It might be related to the fact that, in the western USA, SWE is decreasing at a higher rate in warmer watersheds than that in colder watersheds (Mote, 2006). The disappearance of snow would reduce the contribution of the low-frequency components of streamflow and, by implication increase the contribution of the high-frequency components.

Another temperature related important variable is the trend in AMJ (Apr-May-Jun) maximum daily temperature. This quantity has decreased in most of the watersheds. In the watersheds with a moderate (large) decrease, the F_6 was likely to increase (decrease). It was observed that the *significant* decrease in AMJ maximum daily temperature occurred in watersheds with the aridity index of less than 1.5 (which includes humid watersheds). About 65% of the watersheds with the *moderate* decrease in this quantity were arid. The snow-dominated arid watersheds are primarily located in the western USA. The snow-dominated humid watersheds are primarily located in the eastern USA, the Pacific Northwest, and the Northern Rocky Mountains. Thus, change in AMJ maximum daily temperature has different effects in wet/moderate-dry and dry watersheds. The mechanism behind the effect of AMJ temperature was unclear.

Soil properties that were important in determining the trends in F_6 were sand fraction, silt fraction, soil conductivity, soil depth, and depth to bedrock. Watersheds with sandy and high conductivity soils were more likely to exhibit a decrease in F_6. Watersheds with clayey and low conductivity soils were more likely to exhibit an increase in F_6. One of the differences between the watershed with clayey and sandy soils was that in the former the average high rainfall depth increased more significantly. In the watersheds with clayey soils, the OND (Oct-Nov-Dec) temperatures increased moderately, whereas in the watersheds with sandy soils, the OND temperatures increased significantly. Also note that in most of the snow-dominated watersheds, the high rainfall occurs mainly in the winter season. These observations lead to the following hypothesis. In watersheds with clayey soils, an increase in high rainfall depth together with only a moderate increase in winter maximum daily temperature is responsible for an increase in F_6: moderate increase in winter maximum daily temperature ensures that soil moisture does not decrease significantly. In watershed with sandy soils, a decrease or only a moderate increase in high rainfall depth with a large increase in winter maximum daily temperature is responsible for a significant decrease in soil moisture. This decrease in soil moisture is responsible for the decrease in F_6.

Finally, the trend in δ_{snow} and the trend in time-to-peak are important variables for determining the change in F_6. Higher the increase in δ_{snow}, higher the increase in F_6; higher the decrease in time-to-peak, higher the increase in F_6. Both, the increase in δ_{snow} and the decrease in time-to-peak suggest an increase in snowmelt rate. This, in turn, implies that water is reaching the river network faster, which decreases the contribution of the low-frequency component and increases the F_6 values. In summary, in the snow-dominated watersheds changes in rainfall depth and duration, the increase in winter (OND) and the decrease in spring (AMJ) temperatures, and the change in snowmelt is responsible for the change in F_6.

Figure 10 shows the probability distribution of important variables that determine the change in the contribution of 1-month to 1-year timescale components (F_5) – only the 24 most important variables are shown in the figure. Precipitation related important variables were the trend in high precipitation duration, the trends in mean and median storm depth, and the trend in total storm depth. An increase in mean, median, and total storm depth was associated with a decrease in F_5. High precipitation duration decreased in most of the watersheds. If the decrease in average precipitation duration was large, then the watershed was more likely to exhibit an increase in F_5; if only a moderate decrease or increase in average precipitation duration was observed, the watershed was likely to exhibit a decrease in F_5. As discussed above, changes in precipitation statistics also explained changes in F_6. Basically, an increase in storm depth and an increase in high rainfall duration were related to an increase in the high-frequency components and a decrease in the low-frequency components.

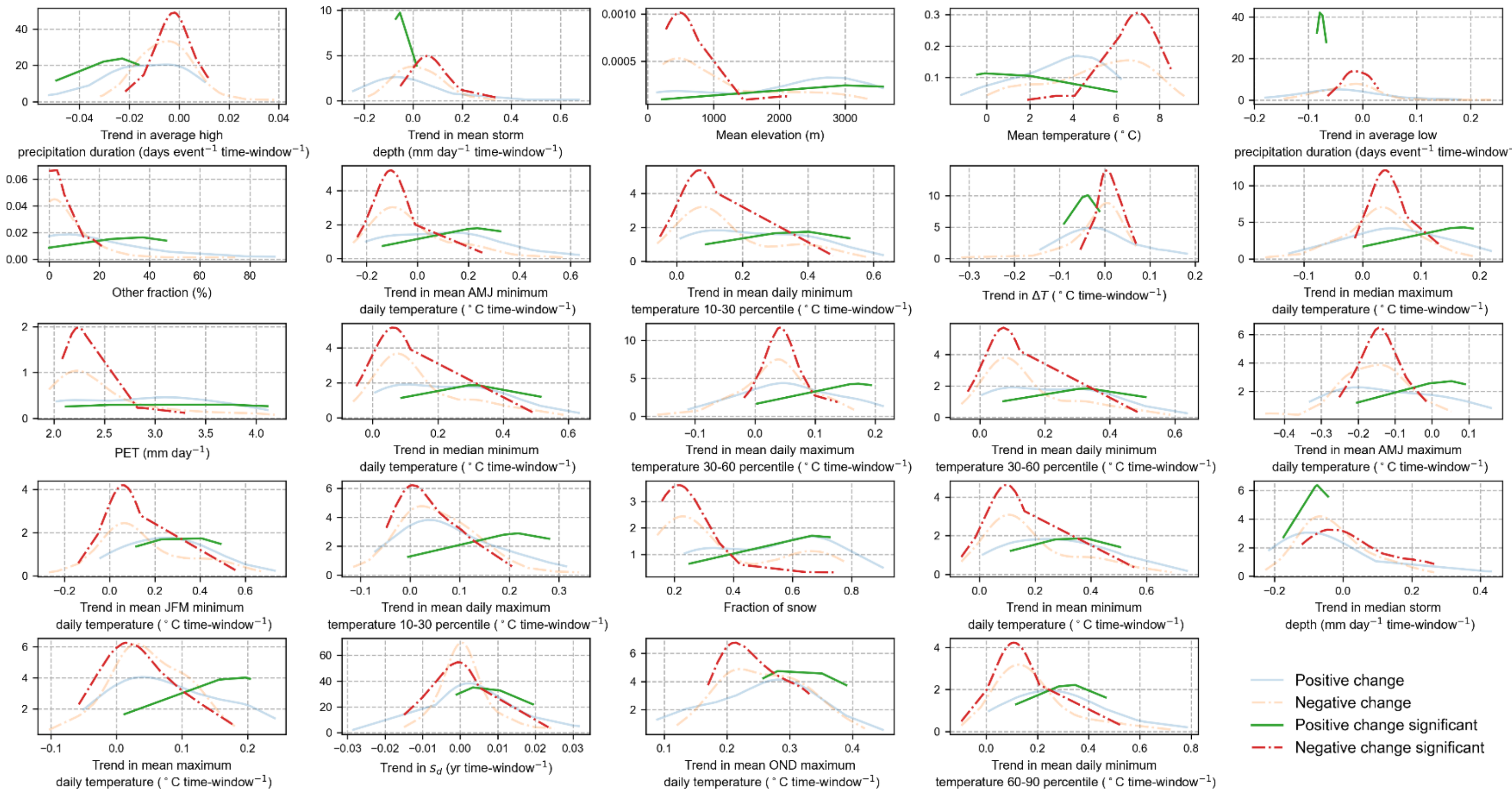

Figure 9. Snow-dominated watersheds. Probability distribution of important predictor variables at less than 1-month timescale. The symbol s_{d} denotes the phase difference monthly rainfall and temperature (see Berghuijs & Woods, 2016 for details).

Mean elevation, mean temperature, and the fraction of snow were also important variables. Watersheds with the lower (higher) mean elevation, the higher (lower) mean temperature, and the smaller (higher) values of the fraction of snow were more likely to exhibit a decrease (increase) in F_5. The threshold value of the fraction of snow at which the sign of change in F_5 transitions from negative to positive is 0.4. The fraction of snow is less than 0.4 in eastern US snow-dominated watersheds and greater than 0.4 for most of the western snow-dominated watersheds (Figure 3 in Addor et al., 2017). This indicates that the change in F_5 is different in the eastern and the western US watersheds which was also observed in Figure 7. Moreover, Figure 7 clearly shows that F_5 ($= F_1 + F_2$) decreased in most of the eastern snow-dominated watersheds while it increased in western snow-dominated watersheds.

Several temperature related variables were important for determining the changes in F_5. Some of these variables include the trends in AMJ minimum and maximum daily temperatures, the trend in mean daily minimum and maximum temperatures, the trend in mean JFM (Jan-Feb-Mar) minimum daily temperature, and the trend in OND maximum daily temperature. Both mean minimum and maximum daily temperatures increased in most of the snow-dominated watersheds.

A moderate increase was associated with a decrease in F_5 and a significant increase was associated with an increase in F_5. As discussed above, an increase in temperature affects the soil moisture regime which, in turn, affects the SSS through changes in the high-frequency components. However, a temperature change can also directly affect the low-frequency components of streamflow, for example, via the changes in the baseflow characteristics, and snowpack storage. These mechanisms have been discussed above.

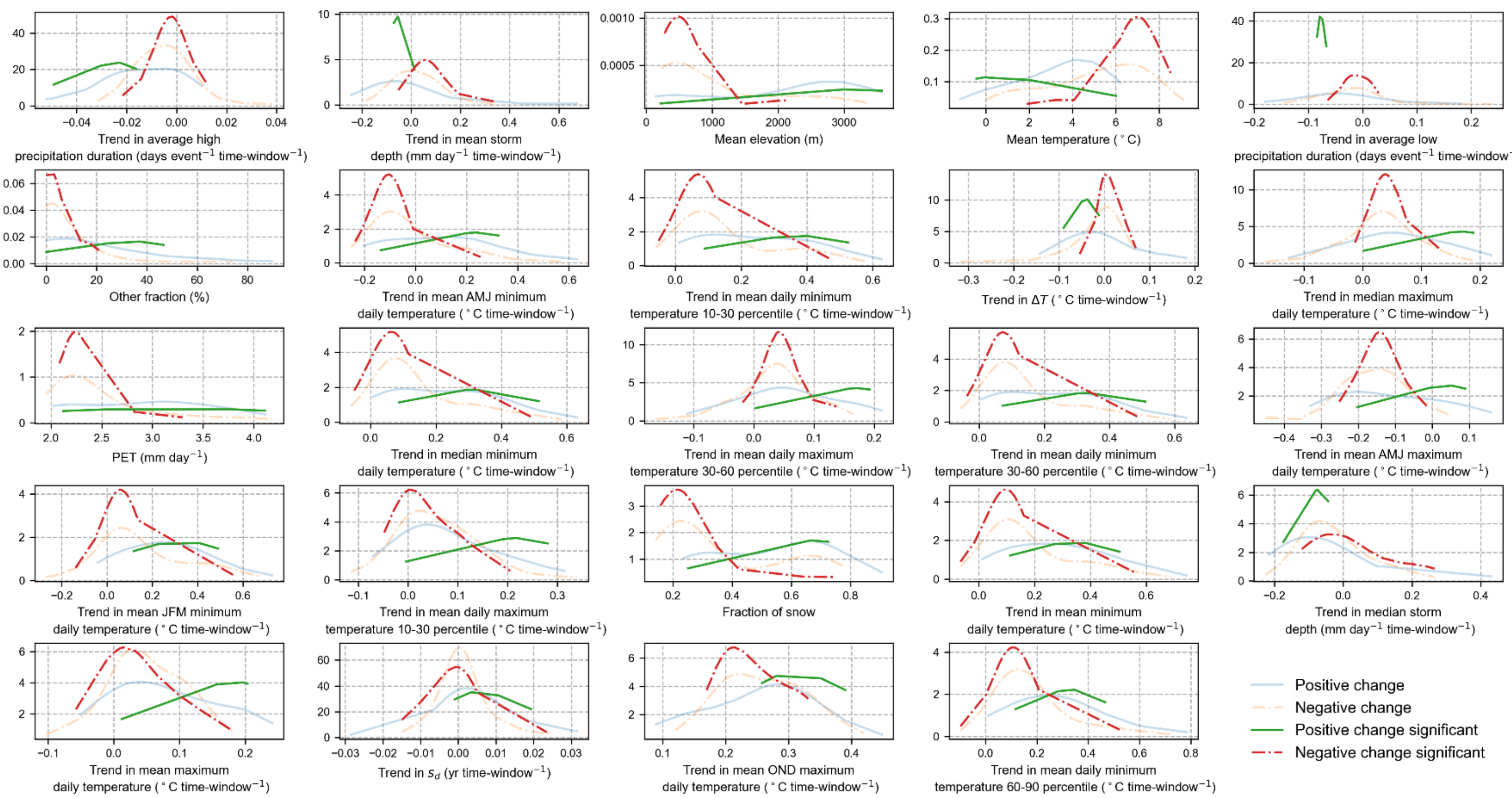

Figure 10. Snow-dominated watersheds. Probability distribution of important predictor variables at 1-month to 1-year timescales. The symbol s_d denotes the phase difference monthly rainfall and temperature (see Berghuijs & Woods, 2016 for details).

7. Causes of SSS changes in the rain-dominated watersheds

In rain-dominated watersheds rainfall is the primary driver of streamflow. Some of the rainwater is intercepted by the plant canopy and other structures, some of the rainwater infiltrates into the soil, and the rest of the rainwater runs off and eventually reaches the rivers. Most of the intercepted rainwater evaporates back to the atmosphere. Some of the infiltrated water goes to groundwater through percolation, some of the infiltrated water goes back to atmosphere in the form of soil evaporation and plant transpiration, and rest of the infiltrated soil water flows below the earth surface to nearby streams which is referred to as interflow. Groundwater also flows to the river, which is referred to baseflow. These processes occur at vastly different timescales and are affected strongly by several watershed properties including their spatial distribution. It is possible that change in the rainfall-runoff response of a watershed is responsible for change in SSS in rain-driven watersheds. In this study, we used a conceptual event-based model to simulate rainfall-runoff response of rain-driven CAMELS watersheds.

The details of the modeling are discussed in SI (Text S4). In summary, hydrograph separation was carried out using streamflow and rainfall data in each of the watersheds (Lamb & Beven, 1997; see Collischonn & Fan et al., 2013 for hydrograph separation). Each rainfall-runoff event was modeled using the SCS-CN method (Ponce & Hawkins, 1996; Mishra & Singh, 1999; Geetha et al., 2007; Soulis & Valiantzas, 2012; Soulis & Valiantzas, 2013) and 2-parameter gamma distribution as unit hydrograph (Botter et al., 2013). There were a total of four model parameters $\lambda, CN, \alpha,$ and β. The first two parameters belong to the SCS-CN model and the last two parameters belong to unit hydrograph. The mean and variance of the unit hydrograph is α/β and α/β^2, respectively. These parameters were estimated for each of the rainfall-runoff event using the Dynamic Dimension Search (DDS) algorithm (Tolson & Shoemaker, 2007) with the objective of minimizing mean-square-error between observed and simulated direct runoff. Once these parameters are obtained for each of the rainfall-runoff events, then the change in these parameters over time can be used as a measure of the change in the rainfall-runoff response of a watershed. One difficulty is that these parameters have high variability from event to event. Therefore, the change in probability distributions of these parameters had to be measured. This was achieved using the moving windows as illustrated in Table 1. All the events contained in a moving window were used to create a probability distribution of the four parameters. The change in probability distribution was measured by estimating the trend in several statistics of the probability distributions which includes mean, mean of 0-10 percentiles, mean of 10-30 percentiles, mean of 30-60 percentiles, mean of 60-90 percentiles, and mean of 90-100 percentiles. The important variables were recognized using the same method as in snow-dominated watersheds.

Figure 11 shows the conditional probability densities of important variables for the classification of positive and negative trends at the less than 1-month timescale (F_6) in rain-dominated watersheds. Some of the important variables are the trend in OND mean maximum daily temperature, the trend in median minimum daily temperature, and the aridity index. The value of F_6 increased in many of the arid watersheds while it decreased in most of the humid watersheds. Further, F_6 increased in the watersheds in which the OND maximum daily temperature increased significantly. It was observed that the arid rain-driven watersheds had a higher increase in OND maximum daily temperature (Figure 4), a higher increase in the number of dry days, and a higher increase in JAS maximum and minimum daily temperature. Also, changes in average rainfall depth in arid watersheds during the OND and JAS months were small (not shown). All these factors indicate that the increase in evaporation was more than the increase in rainfall in the arid watersheds which resulted in a decrease in the low-frequency components of streamflow in these watersheds. And a decrease in low-frequency components is responsible for an increase in high-frequency components. Figure 11 also shows that an increase in median minimum daily temperature is associated with an increase in F_6. This further supports the hypothesis that the decrease in the contribution of the low-frequency components in arid watersheds is due to an increase in evaporation, and subsequent decrease in the low-frequency components.

Many of the humid watersheds where F_6 decreased are located in the Pacific Northwest and the Gulf Coast region where rainfall is more frequent in the winter months. It was observed that the OND rainfall depth decreased in most of the humid watersheds and the OND temperature increased moderately in these watersheds. These two factors can explain the decrease in F_6 in these watersheds. An increase in temperature implies higher potential evaporation and higher actual evaporation (because humid watersheds are energy-limited), and lesser soil moisture. Thus, more rainwater is absorbed by the soils and lesser rainwater reaches the river network in the form of direct runoff. The decrease in rainfall further amplifies this process. Other observations that support this hypothesis are a decrease in the median storm depth and a decrease in high rainfall duration in most of the watersheds. Ficklin et al. (2016) also reported a decrease in quick runoff in several watersheds located in the Pacific Northwest and the Gulf Coast which supports this hypothesis.

The values of F_3 have decreased in almost all the Pacific Northwest watersheds (Figure 7). As discussed above, the value of F_3 is partially determined by ET: an increase in ET results in a decrease in F_3. Therefore, the decrease in F_3 and F_6 in these watersheds suggests an important role of temperature in changing the SSS.

Some of the rainfall related variables such as the trend in low rainfall frequency, the trends in low rainfall duration and frequency, the trend in the number of rain days, the low rainfall frequency, and the mean rainfall were also important. These variables are also related to the aridity and humidity of the watersheds. Watersheds with low mean rainfall and a larger number of dry days are typically arid. In most of the watersheds where the number of rain days decreased, the number of dry days increased, and the low rainfall duration increased, the F_6 value also increased. This is expected because these trends indicate an increase in the aridity of these watersheds – arid watersheds are known to exhibit high values of F_6 (Figure 5). Figure 11 also shows that in most of the watersheds where F_6 has increased, the number of rain days has also decreased.

Some of the soil properties such as sand fraction and the porosity including the fraction of forest are also important variables. Most of the watersheds with sandy and smaller porosity soils and a large fraction of forest cover exhibited a decrease in F_6. These three variables are correlated since sandy soils are known to be porous and ideal to support forests (Eagleson, 1982). It was observed that most of the CAMELS watersheds with sandy soils are located in humid regions with high mean annual rainfall. Thus, the decrease in F_6 in watersheds with sandy soils can be explained as in humid watersheds as discussed above.

Another difference between watersheds with sandy and fine soils was that in the former the phase difference between monthly rainfall and evaporation (s_{d}; see Berghuijs & Woods, 2016 for details) decreased which might have resulted in more rainwater evaporating back to the atmosphere, drying of soils, and muted response of the watersheds to rainstorms. Many of the watersheds in the Pacific Northwest have sandy soil.

One notable point in the above discussion is that the OND maximum temperature has increased in most of the watersheds. In humid watersheds, the increase is moderate, and, in arid watersheds, the increase is large. But this increase has an opposite effect on the SSS in the humid and arid watersheds. In humid watersheds, the increase in the OND temperature resulted in an increase in ET, a decrease in soil moisture, and a muted response of the watershed to rainfall which resulted in a decrease in the high-frequency components. In arid watersheds, the increase in the OND temperature resulted in an increase in ET and a decrease in the low-frequency components which, in turn, resulted in an increase in the high-frequency components. Thus, change in OND temperature directly affects the high-frequency components in humid watersheds and only indirectly affects them in arid watersheds.

One question remains here: Why the high-frequency component is not directly affected by the change in the OND temperature in arid watersheds? The reason is that in the majority of the rain-driven arid watersheds in the USA, rainfall pre-dominantly occurs in spring-summer months (except in California where rain occurs in winter months) (Addor et al., 2017, Fig 3). Thus, an increase in ET in winter months directly affects only the low-frequency component, not the high-frequency component. The high-frequency component is formed by the summer rainfall which appears to be unchanged during the study period. This conclusion is further supported by the fact that the AMJ (Apr-May-Jun) and the JAS (Jul-Aug-Sep) maximum daily temperatures have not increased significantly in these watersheds. The AMJ minimum daily temperature also did not increase in most of the watersheds. The JAS minimum daily temperature increased significantly only in a few of the arid watersheds (<40%). In contrast to arid watersheds, rainfall occurs in winter months in many of the humid watersheds, especially the ones located in the Pacific Northwest. Therefore, the change in temperature directly affects the high-frequency component in humid watersheds.

Finally, two of the parameters of the rainfall-runoff model came out to be important for determining the SSS change: CN and λ. A decrease in CN and an increase in λ seem to be associated with an increase in F_6. This association, however, is weak because several of the watersheds where CN decreased also reported a decrease in F_6. Also, the changes in CN and λ are relatively small in most of the watersheds. Therefore, we conclude that changes in the SSS in the rain-driven watersheds are a direct result of the change in climate statistics rather than the changes in the rainfall-runoff response of the watersheds.

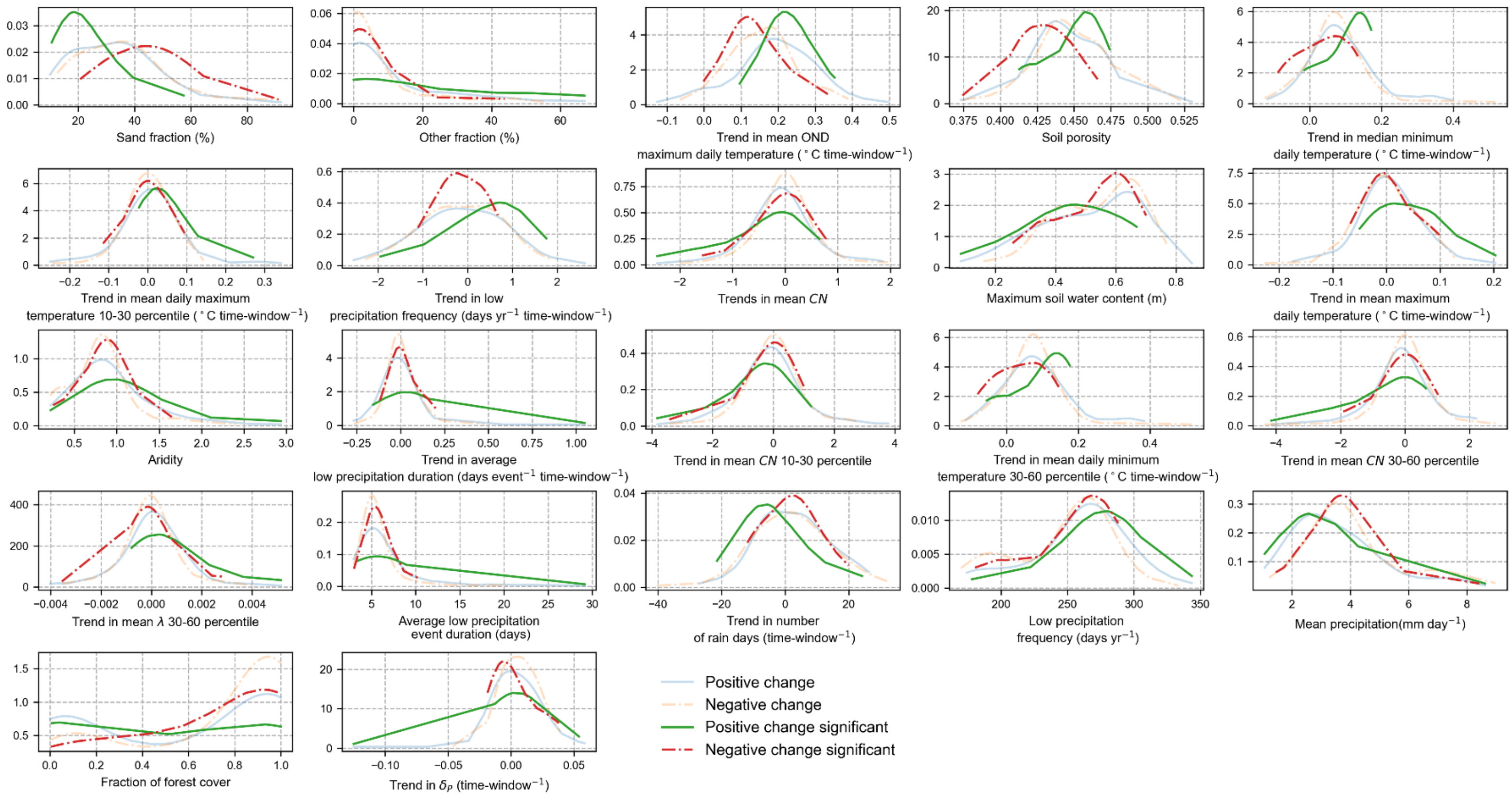

Figure 11. Rain-dominated watersheds. Probability distribution of important predictor variables for classification of positive and negative trends at less than 1-month timescales. The symbol δ_P denotes the amplitude of normalized mean rainfall (see Berghuijs & Woods, 2016 for details).

The causes for change in low-frequency components is not discussed because fluctuation at greater than 1-year timescales had very small contribution to total streamflow variance in rain-dominated watersheds. Therefore, the contribution of 1-month to 1-year timescale components is almost one-to-one related to less than 1-month timescale contribution.

8. Summary and Conclusions

The main conclusions of this study are summarized in Table 2. It was found that the effect of climate change on SSS change was strongly modulated by watershed static attributes. The contribution of greater than 1-year timescales fluctuations to total streamflow variance is typically very small in rain-driven watersheds, but it is substantial in western snow-dominated watersheds where the fraction of snow is greater than 0.4. The contribution of 1-month to 1-year timescale fluctuations strongly depends upon the contribution of baseflow to total streamflow. Also, long-term persistence (value of d) in deseasonalized streamflow time series depends upon the contribution of baseflow: low values of BFI are associated with weaker long-term persistence. The contribution of 2-weeks to 1-month timescale fluctuations to total streamflow variance appears to be determined by interflow and rainfall. The contribution of high-frequency components is mainly determined by the quick flow. Thus, spectral analysis of deseasonalized streamflow time series can be very useful in detecting hydrologic regime changes in a watershed through analysis of streamflow time series.

In snow-dominated watersheds across the USA, a clear east-west divide was found in terms of change in SSS. F_1 and F_2 decreased (increased) in most of the eastern (western) watersheds. F_0 decreased in most of the western watersheds. The high-frequency components increased in most of the snow-dominated watersheds. Increases in high-frequency components and decreases in low-frequency components in snow-dominated watersheds were related to increases in rainfall in these watersheds but also to increases in OND temperatures. It could be concluded that trends in rainfall have significant control over SSS change in snow-dominated watersheds. Changes in snowmelt-temperature relationships also played a role in changing the SSS in snow-dominated watersheds.

In most rain-driven watersheds and in eastern snow-dominated watersheds, the contribution of high-frequency (less than one-month) components was greater than 50%. This was particularly the case in the watersheds in the Great Plains and the Mississippi Valley where the contribution of low-frequency components is very small due to high ET. In most of the arid watersheds, the values of F_4 and F_6 increased. These increases are related to increases in ET in these watersheds in winter months which decreased contributions from low-frequency components and, in turn, increased the contribution of the high-frequency components.

The high-frequency fluctuations, F_6, decreased in the Gulf Coast watersheds and the Pacific Northwestern watersheds. The reason for this was also the increase in winter ET and decrease in winter rainfall depth in these watersheds. In these watersheds, the dominant rainfall season is winter; therefore, an increase in ET possibly resulted in a decrease in antecedent soil moisture and, overall, muted response of watersheds to rainfall. There was a difference in the Pacific Northwest and Gulf Coast watersheds: the values of F_4 increased in the majority of the Pacific Northwest region while they decreased in the latter.

The trends in the contribution of fluctuations at different timescales were also related to soil properties such as soil texture, porosity, and the fraction of forest. Further analyses revealed that soil properties were an indicator of change in climatic statistics. In snow-dominated watersheds with fine soils, high rainfall depth increased, and winter maximum daily temperature increased only moderately. This is hypothesized to have resulted in an increase in F_6 in these watersheds. In the snow-dominated watershed with sandy soils, a decrease or only a moderate increase in high rainfall depth with a large increase in winter maximum daily temperature is hypothesized to result in a significant decrease in soil moisture and a decrease in F_6.

In the rain-dominated watersheds with sandy soil, F_6 decreased. Most of the watersheds with sandy soils are in humid regions with high mean annual rainfall. Another difference between watersheds with sandy and fine soils was that in the former the phase difference between monthly rainfall and evaporation decreased which might have resulted in more rainwater evaporating back into atmosphere, drying of soils, and muted response of watersheds to the rainstorms.

In snow-dominated watersheds change in the temperature-snowmelt relationship is responsible at least to some extent for SSS change. The change in the temperature-snowmelt relationship is likely due to changes in spatiotemporal snow statistics and temperature statistics rather than any physical changes in the watersheds. Although, changes in vegetation density might also be responsible for the changes. In rain-dominated watersheds, the change in the rainfall-runoff relationship appears to be negligible.

We note that conclusions reported in this study apply only to deseasonalized streamflow time series. Changes in seasonal components are not studied in this paper. Nevertheless, the results presented in this study convincingly show that changes in SSS have occurred across the USA. Although the pattern of changes is patchy, there is substantial spatial structure. These changes have consequences for the accurate simulation of streamflow time series in the presence of climate change. Decreasing the influence of low-frequency components can result in a decrease in the accuracy of simulations. This is evident in arid watersheds of the Great Plains where the contribution of low-frequency components has always been small, and all the models (conceptual, process-based, and ML models) of streamflow have been reported to perform poorly in these watersheds (e.g., Konapala et al., 2020).

In this study, only the effect of climatic statistics changes on SSS change has been explored. But SSS can also change due to the natural changes in the land-use such as forest disturbance (e.g., Goeking & Tarboton, 2022). The effects of such changes on SSS should be the topic of future study. Moreover, we believe that it would be worthwhile to simulate the hydrologic response of CAMELS watersheds using a detailed process-based model to understand the changes in various hydrologic quantities in these watersheds.

Finally, the analysis carried out in this study identifies only the variables that play a role in determining the changes in SSS. The specific mechanisms creating the changes could not be identified using this analysis. Nevertheless, a few hypotheses regarding changes in the hydrologic mechanisms that might have led to SSS change have been proposed. Data between water years 1980-2013 was used to achieve the objectives. Though 30-35 years of data are not enough to identify all the changes in SSS, such data can still reveal the useful pattern of hydrologic change (e.g., Ficklin et al., 2016). Besides, it is well known that systematic changes in global temperatures and rainfall patterns have occurred over the study period (Manabe & Broccoli, 2020). Therefore, we believe that it is prudent to look for SSS changes across the USA due to climate change over the period used in this study.

Table 2. A summary of streamflow statistical structure (SSS) and the changes in SSS in different regions of USA

Geographic region	Climate	Streamflow statistical structure	Change in streamflow statistical structure	Cause of change
Pacific Northwest	Humid	High values of F_3, F_5, F_6, low values of F_0	Decrease in F_3 and F_6, increase in F_4 in some of the watersheds	Increase in winter temperature and decrease in winter rainfall depth, resulting in decrease in the strength of interflow seems to be the main cause. Winter is the high rainfall season in these watersheds.
Gulf Coast	Humid	High values of F_6, moderate to high value of F_3 and F_5	Decrease in F_6, F_4, mixed response of change in F_3; Increase in low-frequency components F_0, F_1, and F_2	Decrease in winter temperature and decrease in winter rainfall depth, resulting in muted response of these watersheds to rainfall seems to be the main cause. Winter is the high rainfall season in these watersheds.
Great Plains	Arid	Very high values of F_6. Low to moderate values of F_0, F_3, and F_5	Mixed trends, but majority of the watersheds had increase in high-frequency components and decrease in low-frequency components	Increase in OND temperatures, resulting in increase in ET and decrease in low-frequency components. Spring-summer is the main rainfall season in these watersheds.
Atlantic Coast and eastern most Great Lakes region	Humid	Low value of F_0, high values of F_5 and F_6, low to high values of F_3.	Increase in F_4 and F_6, decrease in F_3 and F_5	Increase in precipitation
Rocky Mountains	Arid	Moderate to high values of F_0, high values of F_5, low values of other components	Decrease in F_0, increase in F_4 and F_6; F_1 and F_2 had both positive and negative trends	Increase in temperature, change in rainfall patterns, and decrease in SWE.
High Plains	Arid	Moderate to high values of F_0, high values of F_5, low values of other components	Mixed trends, F_1 increased in most of the watersheds; F_0 decreased in some and increased in other watersheds	Increase in temperature, change in rainfall patterns, and decrease in SWE. The cause of differences between the High Plains and the western Rocky Mountains is unclear.

F_0 = Fraction of variance contributed by greater 1-year timescale components; F_1 = Fraction of variance contributed by 4-months to 1-year timescale components; F_2 = Fraction of variance contributed by 1-month to 4-months timescale components; F_3 = Fraction of variance contributed by 2-weeks to 1-month timescale components; F_4 = Fraction of variance contributed by less than 2-weeks timescale components;

$F_5 = F_1 + F_2$; $F_6 = F_3 + F_4$

Appendix A:

Table A1. Variables used in the study to interpret the streamflow statistical structure (SSS) changes

Property	Variables	Remarks
Rainfall	Mean rainfall, rainfall seasonality (see Addor et al., 2017), high rainfall frequency, high rainfall duration, low rainfall duration, trend in mean rainfall depth, trend in total rainfall depth, trend in number of rainstorms, trend in number of rain days, trend in high rainfall frequency, trend in high rainfall duration, trend in high rainfall depth, trend in low rainfall frequency, trend in low rainfall duration, trend in low rainfall depth, trend in OND (Oct-Nov-Dec) rainfall depth, trend in JFM (Jan-Feb-Mar) rainfall depth, trend in AMJ (Apr-May-Jun) rainfall depth, trend in JAS (Jul-Aug-Sep) rainfall depth	
Temperature	Mean temperature, trend in mean minimum daily temperature, trend in mean maximum daily temperature, trend in median minimum daily temperature, trend in median minimum daily temperature, trend in median maximum daily temperature, trend in SD (standard deviation) maximum daily temperature, trend in SD minimum daily temperature, trend in OND minimum (maximum) daily temperature, trend in JFM minimum (maximum) daily temperature, trend in AMJ minimum (maximum) daily temperature, trend in JAS minimum (maximum) daily temperature, trend in mean minimum (maximum) daily temperature 0-10 percentiles, trend in mean minimum (maximum) daily temperature 10-30 percentiles, trend in mean minimum (maximum) daily temperature 30-60 percentiles, trend in mean minimum (maximum) daily temperature 60-90 percentiles, trend in mean minimum (maximum) daily temperature 90-100 percentiles,	
Snow statistics	Fraction of snow, trend in snow water equivalent (SWE)	For snow-dominated watersheds
Geomorphological characteristics	Mean elevation, mean slope, drainage area	
Climate indices except precipitation	Potential evapotranspiration (PET), aridity, runoff	
Monthly climate statistics	Temperature amplitude (ΔT), mean normalized rainfall amplitude (δ_{P}), temperature phase (s_{T}), rainfall phase (s_{P}), phase difference between rainfall and temperature (s_{d})	Berghuijs & Woods, (2016)
Soil properties	Soil depth, depth to bedrock, soil conductivity, fraction of sand content, fraction of clay content, fraction of silt	Addor et al., (2017)

	content, fraction of organic content, water holding capacity, other fractions	
Land use	Fraction of forest	
Location	Latitude, Longitude	
Rainfall-runoff response	Trend in λ, CN, α/β, α/β^2 and mean of different percentiles on these quantities	Only for rain-driven watersheds (see SI)
Temperature streamflow relationship	Trend in rising limb slope, trend in rising limb intercept, trend in streamflow regime time-to-peak	Only for snow-dominated watersheds (see SI)

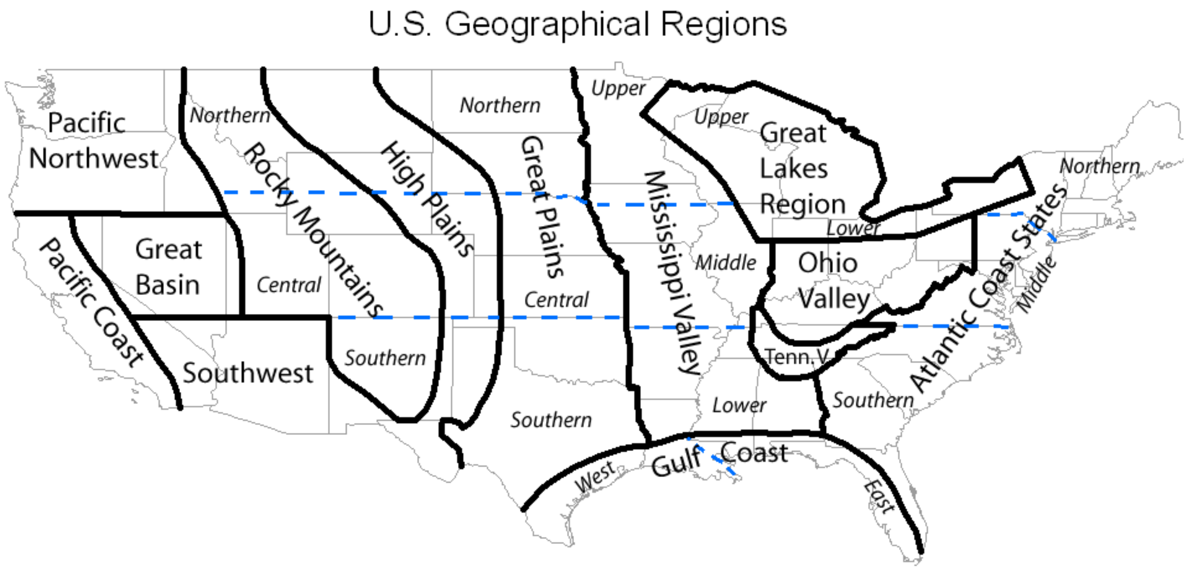

Figure A1. Map of the geographical regions referred to in this study. The details of this map can be found at National Oceanic and Atmospheric Administration (NOAA) through the link (https://www.ncdc.noaa.gov/temp-and-precip/drought/nadm/geography)

Data Availability Statement:

All the data used in this study are publicly available with relevant references provided in the text.

Acknowledgements:

AG was supported by Maki Postdoctoral Fellowship at DRI to carry out this work. Authors acknowledge the feedback from Chris Pearson, and Patrick Sawyer on this work. Authors thank Jaideep Ray for suggesting some of the methodology implemented in the paper and providing feedback on a draft of this paper.

Funding Sources:

This research did not receive any specific grant from funding agencies in the public, commercial, or not-for-profit sectors.

References:

Addor, N., Newman, A. J., Mizukami, N., & Clark, M. P. (2017). The CAMELS data set: catchment attributes and meteorology for large-sample studies. *Hydrology and Earth System Sciences*, 21(10), 5293-5313.

Addor, N., Newman, A., Mizukami, M., & Clark, M. P. (2017). Catchment attributes for large-sample studies. Boulder, CO: UCAR/NCAR. https://doi.org/10.5065/D6G73C3Q

Bárdossy, A., & Anwar, F. (2022). Why our rainfall-runoff models keep underestimating the peak flows? *Hydrology and Earth System Sciences Discussions*, 1-30.

Belmecheri, S., Babst, F., Wahl, E. R., Stahle, D. W., & Trouet, V. (2016). Multi-century evaluation of Sierra Nevada snowpack. *Nature Climate Change*, 6(1), 2-3.

Berg, N., & Hall, A. (2017). Anthropogenic warming impacts on California snowpack during drought. *Geophysical Research Letters*, 44(5), 2511-2518.

Berghuijs, W. R., & Woods, R. A. (2016). A simple framework to quantitatively describe monthly precipitation and temperature climatology. *International Journal of Climatology*, 36(9), 3161-3174.

Betterle, A., Schirmer, M., & Botter, G. (2019). Flow dynamics at the continental scale: Streamflow correlation and hydrological similarity. *Hydrological Processes*, 33(4), 627-646.

Beven, K. J. (2011). Rainfall-runoff modelling: the primer. John Wiley and Sons

Beven, K., & Smith, P. (2015). Concepts of information content and likelihood in parameter calibration for hydrological simulation models. *Journal of Hydrologic Engineering*, *20*(1), A4014010.

Boisramé, G., Thompson, S., Collins, B., & Stephens, S. (2017). Managed wildfire effects on forest resilience and water in the Sierra Nevada. *Ecosystems*, *20*(4), 717-732.

Botter, G., Basso, S., Rodriguez-Iturbe, I., & Rinaldo, A. (2013). Resilience of river flow regimes. *Proceedings of the National Academy of Sciences*, 110(32), 12925-12930.

Box, G. E., Jenkins, G. M., Reinsel, G. C., & Ljung, G. M. (2015). *Time series analysis: forecasting and control*. John Wiley and Sons.

Bras, R. L., & Rodriguez-Iturbe, I. (1993). *Random functions and hydrology*. Courier Corporation.

Breiman, L. (2001). Random forests. *Machine Learning*, *45*(1), 5-32.

Chow, V. T. (1978). Stochastic modeling of watershed systems [French Broad River Basin, North Carolina as an example]. *Advances in Hydroscience Volume 11*, pp. 1-93.

Cleveland, W. S. (1979). Robust locally weighted regression and smoothing scatterplots. *Journal of the American Statistical Association*, 74(368), 829-836.

Collischonn, W., & Fan, F. M. (2013). Defining parameters for Eckhardt's digital baseflow filter. *Hydrological Processes*, 27(18), 2614-2622.

Donohue, R. J., Roderick, M. L., McVicar, T. R., & Farquhar, G. D. (2013). Impact of CO2 fertilization on maximum foliage cover across the globe's warm, arid environments. *Geophysical Research Letters*, 40(12), 3031-3035.

Eagleson, P. S. (1982). Ecological optimality in water-limited natural soil-vegetation systems: 1. Theory and hypothesis. *Water Resources Research*, 18(2), 325-340.

Dlugokencky, E. and Tans, P. NOAA/GML (gml.noaa.gov/ccgg/trends/), date accessed: 17 Mar 2022.

Ficklin, D. L., Robeson, S. M., & Knouft, J. H. (2016). Impacts of recent climate change on trends in baseflow and stormflow in United States watersheds. *Geophysical Research Letters*, 43(10), 5079-5088.

Geetha, K., Mishra, S. K., Eldho, T. I., Rastogi, A. K., & Pandey, R. P. (2007). Modifications to SCS-CN method for long-term hydrologic simulation. *Journal of Irrigation and Drainage Engineering*, 133(5), 475-486.

Goeking, S. A., & Tarboton, D. G. (2021). Variable streamflow response to forest disturbance in the western US: A large-sample hydrology approach. *Water Resources Research*, e2021WR031575.

Gordon, B. L., Brooks, P. D., Krogh, S. A., Boisrame, G. F., Carroll, R. W., McNamara, J. P., & Harpold, A. A. (2022). Why does snowmelt-driven streamflow response to warming vary? A data-driven review and predictive framework. *Environmental Research Letters*, 17 053004.

Granger, C. W. (1980). Long memory relationships and the aggregation of dynamic models. *Journal of Econometrics*, *14*(2), 227-238.

Granger, C. W., & Joyeux, R. (1980). An introduction to long-memory time series models and fractional differencing. *Journal of Time Series Analysis*, 1(1), 15-29.

Gudmundsson, L., Tallaksen, L. M., Stahl, K., & Fleig, A. K. (2011). Low-frequency variability of European runoff. *Hydrology and Earth System Sciences*, 15(9), 2853-2869.

Hirpa, F. A., Gebremichael, M., & Over, T. M. (2010). River flow fluctuation analysis: Effect of watershed area. *Water Resources Research*, 46(12).

Horner, I., Branger, F., McMillan, H., Vannier, O., & Braud, I. (2020). Information content of snow hydrological signatures based on streamflow, precipitation and air temperature. *Hydrological Processes*, 34(12), 2763-2779.

Hurst, H. E. (1951). Long-term storage capacity of reservoirs. *Transactions of the American Society of Civil Engineers*, 116(1), 770-799.

Kim, D. H., Rao, P. S. C., Kim, D., & Park, J. (2016). 1/f noise analyses of urbanization effects on streamflow characteristics. *Hydrological Processes*, 30(11), 1651-1664.

Klemeš, V. (1978). Physically based stochastic hydrologic analysis. *In Advances in Hydroscience* (Vol. 11, pp. 285-356). Elsevier.

Klemeš, V. (1986). Operational testing of hydrological simulation models. *Hydrological Sciences* Journal, 31(1), 13-24.

Knowles, N., Dettinger, M. D., & Cayan, D. R. (2006). Trends in snowfall versus rainfall in the western United States. *Journal of Climate*, 19(18), 4545-4559.

Kratzert, F., Klotz, D., Brenner, C., Schulz, K., & Herrnegger, M. (2018). Rainfall–runoff modelling using long short-term memory (LSTM) networks. *Hydrology and Earth System Sciences*, 22(11), 6005-6022.

Laio, F., Porporato, A., Ridolfi, L., & Rodriguez-Iturbe, I. (2001). Plants in water-controlled ecosystems: active role in hydrologic processes and response to water stress: II. Probabilistic soil moisture dynamics. *Advances in Water Resources*, 24(7), 707-723.

Lamb, R., & Beven, K. (1997). Using interactive recession curve analysis to specify a general catchment storage model. *Hydrology and Earth System Sciences*, 1(1), 101-113.

Lee, H. T., & Delleur, J. W. (1972). A program for estimating runoff from indiana watersheds, part iii: analysis of geomorphologic data and a dynamic contributing area model for runoff estimation. https://docs.lib.purdue.edu/cgi/viewcontent.cgi?article=1025&context=watertech

Manabe, S., & Broccoli, A. J. (2020). *Beyond global warming: How numerical models revealed the secrets of climate change*. Princeton University Press.

Milly, P. C. D. (1997). Sensitivity of greenhouse summer dryness to changes in plant rooting characteristics. *Geophysical Research Letters*, 24(3), 269-271.

Milly, P. C., & Dunne, K. A. (2016). Potential evapotranspiration and continental drying. *Nature Climate Change*, 6(10), 946-949.

Milly, P. C., Betancourt, J., Falkenmark, M., Hirsch, R. M., Kundzewicz, Z. W., Lettenmaier, D. P., & Stouffer, R. J. (2008). Stationarity is dead: whither water management? *Science*, 319(5863), 573-574.

Milly, P. C., Dunne, K. A., & Vecchia, A. V. (2005). Global pattern of trends in streamflow and water availability in a changing climate. *Nature*, 438(7066), 347-350.

Mishra, S. K., & Singh, V. P. (1999). Another look at SCS-CN method. *Journal of Hydrologic Engineering*, 4(3), 257-264.

Montanari, A., Rosso, R., & Taqqu, M. S. (1997). Fractionally differenced ARIMA models applied to hydrologic time series: Identification, estimation, and simulation. *Water Resources Research*, 33(5), 1035-1044.

Montanari, A., Rosso, R., & Taqqu, M. S. (2000). A seasonal fractional ARIMA model applied to the Nile River monthly flows at Aswan. *Water Resources Research*, 36(5), 1249-1259.

Mote, P. W. (2006). Climate-driven variability and trends in mountain snowpack in western North America. *Journal of Climate*, 19(23), 6209-6220.

Mote, P. W., Hamlet, A. F., Clark, M. P., & Lettenmaier, D. P. (2005). Declining mountain snowpack in western North America. *Bulletin of the American Meteorological Society*, 86(1), 39-50.

Mote, P. W., Li, S., Lettenmaier, D. P., Xiao, M., & Engel, R. (2018). Dramatic declines in snowpack in the western US. *Npj Climate and Atmospheric Science*, 1(1), 1-6.

Mudelsee, M. (2007). Long memory of rivers from spatial aggregation. *Water Resources Research*, *43*(1)

Ponce, V. M., & Hawkins, R. H. (1996). Runoff curve number: Has it reached maturity? *Journal of Hydrologic Engineering*, 1(1), 11-19.

Porporato, A., Laio, F., Ridolfi, L., & Rodriguez-Iturbe, I. (2001). Plants in water-controlled ecosystems: active role in hydrologic processes and response to water stress: III. Vegetation water stress. *Advances in Water Resources*, 24(7), 725-744.

Priestley, M. B. (1982). *Spectral analysis and time series: probability and mathematical statistics* (No. 04; QA280, P7.).

Rodriguez-Iturbe, I., Porporato, A., Laio, F., & Ridolfi, L. (2001). Plants in water-controlled ecosystems: active role in hydrologic processes and response to water stress: I. Scope and general outline. *Advances in Water Resources*, 24(7), 695-705.

Rodriguez-Iturbe, I., Porporato, A., Ridolfi, L., Isham, V., & Coxi, D. R. (1999). Probabilistic modelling of water balance at a point: the role of climate, soil and vegetation. *Proceedings of the Royal Society of London. Series A: Mathematical, Physical and Engineering Sciences*, 455(1990), 3789-3805.

Singh, R., Wagener, T., Van Werkhoven, K., Mann, M. E., & Crane, R. (2011). A trading-space-for-time approach to probabilistic continuous streamflow predictions in a changing climate–

accounting for changing watershed behavior. *Hydrology and Earth System Sciences*, 15(11), 3591-3603.

Sivapalan, M., Yaeger, M. A., Harman, C. J., Xu, X., & Troch, P. A. (2011). Functional model of water balance variability at the catchment scale: 1. Evidence of hydrologic similarity and space-time symmetry. *Water Resources Research*, 47(2)

Soulis, K. X., & Valiantzas, J. D. (2012). SCS-CN parameter determination using rainfall-runoff data in heterogeneous watersheds–the two-CN system approach. *Hydrology and Earth System Sciences*, 16(3), 1001-1015.

Soulis, K. X., & Valiantzas, J. D. (2013). Identification of the SCS-CN parameter spatial distribution using rainfall-runoff data in heterogeneous watersheds. *Water Resources Management*, 27(6), 1737-1749.

Stephens, C. M., Marshall, L. A., Johnson, F. M., Lin, L., Band, L. E., and Ajami, H. (2020). Is past variability a suitable proxy for future change? A virtual catchment experiment. *Water Resources Research*, 56(2), e2019WR026275.

Tessier, Y., Lovejoy, S., Hubert, P., Schertzer, D., & Pecknold, S. (1996). Multifractal analysis and modeling of rainfall and river flows and scaling, causal transfer functions. *Journal of Geophysical Research: Atmospheres*, 101(D21), 26427-26440.

Yang, G., & Bowling, L. C. (2014). Detection of changes in hydrologic system memory associated with urbanization in the Great Lakes region. *Water Resources Research*, 50(5), 3750-3763.

Wu, S., Zhao, J., Wang, H., & Sivapalan, M. (2021). Regional patterns and physical controls of streamflow generation across the conterminous United States. *Water Resources Research*, *57*(6), e2020WR028086.

Zaerpour, M., Hatami, S., Sadri, J., & Nazemi, A. (2021). A global algorithm for identifying changing streamflow regimes: application to Canadian natural streams (1966–2010). *Hydrology and Earth System Sciences*, *25*(9), 5193-5217.